INFORMATION TO USERS

This manuscript has been reproduced from the microfilm master. UMI films the text directly from the original or copy submitted. Thus, some thesis and dissertation copies are in typewriter face, while others may be from any type of computer printer.

The quality of this reproduction is dependent upon the quality of the copy submitted. Broken or indistinct print, colored or poor quality illustrations and photographs, print bleedthrough, substandard margins, and improper alignment can adversely affect reproduction.

In the unlikely event that the author did not send UMI a complete manuscript and there are missing pages, these will be noted. Also, if unauthorized copyright material had to be removed, a note will indicate the deletion.

Oversize materials (e.g., maps, drawings, charts) are reproduced by sectioning the original, beginning at the upper left-hand corner and continuing from left to right in equal sections with small overlaps.

ProQuest Information and Learning
300 North Zeeb Road, Ann Arbor, MI 48106-1346 USA
800-521-0600

NOTE TO USERS

This reproduction is the best copy available.

UMI

THERMAL EXPANSION OF RARE EARTH METALS

by

Fred Barson

A Dissertation Submitted to the
Graduate Faculty in Partial Fulfillment of
The Requirements for the Degree of
DOCTOR OF PHILOSOPHY

Major Subject: Physics

Approved:

IOWA STATE COLLEGE LIBRARY

Signature was redacted for privacy.

In Charge of Major Work

Signature was redacted for privacy.

Head of Major Department

Signature was redacted for privacy.

Dean of Graduate College

Iowa State College

1956

UMI Number: DP11988

UMI®

UMI Microform DP11988

Copyright 2005 by ProQuest Information and Learning Company.
All rights reserved. This microform edition is protected against
unauthorized copying under Title 17, United States Code.

ProQuest Information and Learning Company
300 North Zeeb Road
P.O. Box 1346
Ann Arbor, MI 48106-1346

TABLE OF CONTENTS

T12123

TABLE OF CONTENTS (continued)

INTRODUCTION

Purpose of the Investigation

In recent years rare earth metals have become available in good purity and in sufficient quantity to make possible fairly reliable measurements of their intrinsic properties. There is some evidence that even slight amounts of impurities may cause serious changes in their physical properties, so that the development of efficient methods for the separation and reduction of these metals has been a necessary first step.

These elements are of particular interest, in the long-range view, in that their electronic configurations vary from one metal to the other in most cases only by the number of electrons in the 4f shell. Hence, the hope is that a study of the properties of these metals, as a group, and of the differences between their properties might supply information leading to a better understanding of metals in terms of their electronic structures.

From a more immediate viewpoint, the present investigation was concerned with detecting solid state transformations of these metals, as well as determining quantitative values for their thermal expansion. Properly conducted, dilatometric measurements offer a very sensitive method of detecting transitions and are recognized as one of the principal tools in the investigation of metals. Since such

measurements can be made at very slow rates of warming and cooling, they may disclose certain sluggish or very slight effects not readily found by some other means such as thermal analysis.

It was also hoped, in particular, to clarify certain high temperature transitions which had already been detected in several of these metals: lanthanum, cerium, praseodymium, neodymiun, and ytterbium. Large effects in the electrical resistivity measurements and thermal analyses had disclosed these transformations, but an attempt to determine the crystal structure of the high temperature form failed due to the extremely diffuse nature of the X-ray diffraction patterns. It was believed that a dilatometric study might cast some light on these effects.

Since the rare earth metals are very reactive chemically at high temperatures, and since their thermal expansions turn out to be rather small compared to those of other metals, a sensitive and somewhat specialized dilatometer was required. An appreciable part of the present work was the design of a suitable piece of equipment, which will be described in some detail.

Comments on Thermal Expansion

The coefficient of linear expansion of a substance is defined as its change in length, per unit length, per unit change in temperature. Symbolically, this is written

$$\alpha = \frac{1}{L}\frac{dL}{dt}$$

Since for most metals α is on the order of 10^{-5} $^{\circ}C^{-1}$, the length does not change greatly even for rather large temperature intervals. Hence it is common to re-define the coefficient as

$$\alpha = \frac{1}{L_o}\frac{dL}{dt}$$

where L_o is the length at room temperature or at some other convenient temperature such as 0°C. This new definition does not make an appreciable change in the value of α and simplifies the calculations considerably.

There have been several relationships observed between the thermal expansion of a substance and its other physical properties. Of these, the most famous is undoubtedly the relationship derived by Grüneisen and bearing his name (1):

$$\frac{3\alpha V}{C_v k} = \gamma$$

where C_v is the specific heat at the constant volume V of the substance, k is its compressibility, and γ is a pure number, called the Grüneisen constant, which is usually between 1.5 and 2.5 for a metal. The quantity 3α should more properly be replaced by the coefficient of cubical (or volume) expansion; however, for an isotropic substance the volume coefficient is readily shown to be equal to three times the linear expansion coefficient.

Several authors have derived empirical relationships involving the thermal expansion of a metal and its melting point. In general the lower melting metals have greater expansion coefficients, as if a certain percentage expansion brings about the weakening of bonds associated with melting. In particular, Bonfiglioli and Montalenti (2) pointed out that for metals of a certain crystalline form the product of the thermal expansion and the melting point temperature tended to be a constant which was somewhat different from the similar constant for other crystal classes. Although there was some deviation from this grouping and some overlapping of groups, it may be of interest to compare values obtained for the rare earth metals with the constants so obtained for other metals. One would also be interested in testing the applicability of Grüneisen's law to the physical constants of this group of elements, wherever the required constants have been determined.

REVIEW OF LITERATURE

Dilatometric Methods

Since the literature on dilatometry has become voluminous, the reader is referred to a review article by Hidnert and Souder (3) for a summary of the types of dilatometers commonly used and for an extensive list of references. It might be well to describe some of these dilatometers here, however, in order to compare them to the apparatus used in the present investigation and to give some feeling for the experimental difficulties involved. The following has been extracted largely from the review article mentioned above.

Briefly, the difficulties in dilatometric work are of two types: first, that the effect to be measured is very small, the change in length corresponding to a temperature change of one degree being only about 0.002 per cent; and second, that sample holders and detecting equipment also have expansions which must be either eliminated from the measurements somehow, or allowed for in the calculations.

The so-called precision micrometric method is said to be the most precise known means of measuring thermal expansion. In this apparatus the position of the ends of the sample is indicated by fine wires, weighted and hanging from the ends of the sample. Two micrometer microscopes, mounted on a comparator and separated by a distance approximately equal to the sample length, indicate changes in the sample

length by recording changes in the positions of the vertical wires hanging from the sample. The sample can be heated in a furnace to high temperatures, or cooled below room temperature in liquid baths. This method has the advantage of being an absolute measurement; that is, the changes in length are determined directly, with no corrections for the sample holder, etc., being required. For best results, however, this equipment requires relatively long samples, up to as much as 50cm in length. Samples as short as 10cm may be used, but with a corresponding decrease in sensitivity.

The Fizeau-Pulfrich interferometric dilatometer employs two transparent fused silica (quartz) optical flats which are separated by a small sample in the shape of a ring or a tripod. The sample dimensions are adjusted so as to place the optically flat surfaces at a very slight angle to each other, about 20' of arc. Illumination of these flats with monochromatic light produces interference fringes which move across the field of view as the distance between the optical flats changes. Since this distance is exactly the sample length, the method permits a sensitive determination of the thermal expansion of the sample simply by counting the number of fringes passing a fixed point during a measured temperature interval. To eliminate the need for constant observation of the fringes, methods have been developed to record their passage photographically or by means of a photo-tube and counter. The Fizeau-Pulfrich method is particularly

useful when only small lengths of material are available, such as single crystals. Conversely, it has the disadvantage that only very small samples can be used, for if the sample length exceeds about 1cm, satisfactory interference fringes cannot be produced. The measurement is, however, an absolute one once again.

A third type of dilatometer is the fused-quartz tube and dial-indicator apparatus. In this case, a 20cm sample is placed in a fused-quartz (silica) tube which has been sealed at the bottom. A movable fused-quartz rod, resting upon the sample, transmits the motion due to the expansion of the sample to a dial-indicator gauge at the open top of the tube. This method is not absolute, since the readings of the dial-indicator register the differential expansion of the sample relative to an equal length of fused quartz. A small correction must be added to account for this. As described, this method requires relatively long samples and is capable of an accuracy of about 2 per cent in the optimum case.

The autographic optical-lever method employs a mirror supported by a tripod, one leg of which is fused silica, one leg the sample itself, and one leg a Chromel A rod. The fused silica rod, with its very small expansion, acts as a "fixed point" to support one corner of the mirror in a practically stationary position. The rod of Chromel A, which has an expansion practically linear with temperature, tilts the mirror through an angle proportional to the temperature

at any time. Expansion of the sample, which supports the mirror at a third point, tilts the mirror through a second angle which is proportional to the change in sample length. These three legs are arranged so that the tilting due to the sample expansion will be at right angles to that due to the Chromel. A spot of light focused on the mirror and reflected to a glass screen indicates, thus, the expansion of both the Chromel and the sample and describes a curve as the temperature changes. The ordinate of this curve represents the expansion of the sample, and the abscissa the expansion of the Chromel, or the temperature. If a photographic plate is substituted for the glass screen, an expansion curve can be plotted directly. This method is not an absolute one, and is only some 3 to 5 per cent accurate. However, it is fast and automatic and leaves a permanent and continuous record.

Electronic methods of recording changes in length have also been developed. In these, the sample is arranged so that its expansion moves one plate of a capacitor, thus varying the series grid capacitance of an oscillator circuit. Alternatively, the iron core of a small transformer may be moved by the expansion of the sample, changing the output voltage markedly while the input voltage is kept constant. Either of these methods can be made extremely sensitive electronically, but still suffer the same disadvantage of other equipment: namely that either the motion of the expansion must be transmitted by some mechanical device to the

transformer or capacitor, or that these detecting devices must be placed within the furnace or cryostat where their own expansion may affect the results. These devices are, thus, not absolute, but are capable of high sensitivity if properly calibrated.

The thermal expansion of crystals, including metals, of course, can also be inferred from X-ray crystallographic measurements by determining the change in the lattice parameters at different temperatures. Due to the small value of the thermal expansion, extremely accurate lattice parameters must be obtained, and the method is not very sensitive except where large temperature changes are involved. The advantages are the facts that extremely small samples may be used, and, even more important, that any anisotropy in the expansion of the crystal becomes immediately evident.

Finally, by determining the density of a sample at different temperatures, one may calculate its cubical expansion. The densities may be found by weighing the sample at different temperatures in air and in a liquid whose density is well known over the temperature range of interest. Small, irregularly-shaped samples may be used in this way, but the method is obviously limited by the availability of a suitable liquid.

Properties of Rare Earth Metals

In reviewing the literature on the rare earth metals, there has once more been the necessity of abbreviating somewhat in order to keep the review of a reasonable length. In general, an effort has been made to include comments directly connected with phase transitions or other unusual behavior in the properties of these metals, with emphasis being placed on data in the high temperature region in particular. The crystal structures of each is included in the description of the metals, and some mention made of particularly unusual or interesting properties in the low temperature region.

Lanthanum

A review of the findings of many investigators on the crystal structure of lanthanum has been given by Herrmann (4, p.13). Several found the room temperature form to be hexagonal close-packed, while several others found only face-centered cubic. Annealing above 350°C seemed to favor formation of the cubic form. Herrmann (4, p.47) reported the room temperature form of lanthanum as hexagonal close-packed, but with the c_o dimension twice that found by others, that is, with a stacking sequence ABAC... rather than the usual ABAB....

The melting point of lanthanum was given as 915°C by Vogel and Heumann (5), who also reported a solid state transformation at about 830°C. Massenhausen (6), employing thermal analysis on a slightly impure sample of lanthanum, gave

the melting point as 863°C, but significantly also found a second thermal arrest at 812°C. More recently, Vogel and Klose (7) found the melting point of a 97 per cent lanthanum sample at 865°C, with a transformation at 775°C, and a second, presumably the hexagonal close-packed to face-centered cubic transition, at 300° - 350°C. Spedding and Daane (8) reported the melting point to be 920°C, and the temperature of the solid state transformation to be 868°C.

The electrical resistivity of lanthanum at low temperatures was studied by many investigators, since this metal was found to become superconducting below about 5°K (9, 10). Data on the resistivity in the higher temperature region, however, are more pertinent here. Jaeger, Bottema, and Rosenbohm (11), using 98.8 per cent lanthanum with 1 per cent iron as an impurity, found anomalies indicated by their resistivity date at 420° - 436°C, 560°C, and 709° - 715°C. These investigators also found specific heat anomalies at 548°C, 655°C, and 709°C, and concluded that this metal consisted, at any temperature, of a mixture of at least two of four possible allotropic phases. Herrmann (4, p.120), who measured the electrical resistivity at high temperatures of a sample of quite pure lanthanum, found a considerable anomaly at 860° - 868°C. Apparently corresponding to the high temperature transformation found by thermal analyses, this anomaly consisted of a sudden change in the resistivity by some 10 per cent of its value at those temperatures, the higher

temperature form having the greater resistivity. A second anomaly, found by the same author, appeared as a hysteresis loop in the resistivity-temperature curve between 300°C and 450°C. This effect was larger in the warming direction than in cooling, and became progressively less pronounced with repeated cycling.

Previous dilatometric work was done by Trombe and Foex (12) on a 99.2 per cent lanthanum rod. Their apparatus consisted of a micro-Chevenard dilatometer, an optical-lever type. The coefficient of linear expansion was reported as 2×10^{-6} °C^{-1} at -195°C, 5.8×10^{-6} °C^{-1} at room temperature, and over 7×10^{-6} °C^{-1} at 425°C. Above 650°C, some softening of the sample occurred, so that the run could not be continued higher. A transition, with hysteresis, was noted between 150°C (on cooling) and 350°C (on warming). The higher temperature form was slightly more dense, its formation being marked by a decrease in volume of 0.19 per cent. Barson, Legvold, and Spedding (13) performed measurements of the expansion of lanthanum at low temperatures and found the expansion coefficient to increase smoothly from 4×10^{-6} °C^{-1} at -175°C to 5×10^{-6} °C^{-1} at room temperature.

Bridgman (14) measured the volume compressibility of lanthanum at room temperature and found an abrupt volume decrease of 0.26 per cent at a pressure of 23,370 kg/cm^2. The same investigator found a cusp in the electrical resistivity at about this pressure (15), the more dense form having the lower resistivity.

Cerium

Herrmann's resume of crystallographic work on cerium metal (4, p.18) indicates that the stable form at room temperature is face-centered cubic, although some authors have reported a mixture of hexagonal close-packed cerium along with this form. Under 15,000 atmospheres of pressure, still another modification appeared. Lawson and Tang (16) determined this to be face-centered cubic still, but with a reduced lattice parameter corresponding to a volume decrease of over 16 per cent from the normal form. Schuch and Sturdivant (17) showed that this condensed form could also be obtained by cooling the cerium to low temperatures, their X-ray crystallographic study being made at -195°C. At a suggestion from Linus Pauling, these authors attributed the transition to the passage of a 4f electron to a 5d state.

Studies of cerium in the low temperature range indicated that the transition involves a hysteresis over a considerable temperature interval, and is accompanied by large changes in other physical properties.

Owen (18), for example, found a sudden decrease in the magnetic susceptibility below about -110°C. Trombe (19) observed the hysteresis of this phenomenon, the change in susceptibility occurring at -153°C on cooling and at about -106°C on warming. La Blanchetais (20) confirmed these results on cerium containing only 0.005 per cent iron, showing that the phenomenon was apparently not connected with the presence of ferromagnetic material in the sample.

A hysteresis loop similar to that described above was found in the electrical resistivity curve for cerium as reported by Foex (21) and by James, Legvold, and Spedding (22). The Hall effect, as reported by Kevane, Legvold, and Spedding (23), showed a similar effect, as did the atomic heat determinations of Parkinson, Simon, and Spedding (24).

The dilatometric study of cerium by Trombe and Foex (12) showed a complex behaviour too. For metal which was quenched from high temperatures to room temperature, the low temperature study showed a 10 per cent volume contraction with the familiar hysteresis corresponding to the face-centered cubic to condensed face-centered cubic transition. On the other hand, a slow cooling cycle from high temperatures to low temperatures and returning not only failed to produce the strong contraction at low temperatures, but actually decreased by 0.7 per cent the room temperature density of the sample after cycling. The form of cerium metal so resulting was called by Trombe and Foex the β -state and apparently corresponds to the hexagonal close-packed form. The β -state and the α-state (their notation for the condensed face-centered cubic) were found unable to transform from one to the other at low temperatures, but either could be formed by proper cooling from the γ-state (normal face-centered cubic) at elevated temperatures. The coefficient of expansion was described as being essentially the same as that of lanthanum, outside of the regions of transformation.

Cerium also exhibits anomalous behaviour in the high temperature region, with some evidence of a strong effect of impurities in changing the temperatures of transitions. Loriers (25) employed differential thermal analysis to a sample of 99.6 per cent cerium with an iron content of only 0.005 per cent. He detected transition temperatures of 635°C, 715°C, and 730°C, plus the melting point at 815°C. A sample containing 0.22 per cent iron showed transitions at 540°C, 710°C, and 750°C. Loriers attributed the lower transformation temperatures reported by Vogel (26), Hanaman (27), and Jaeger, Bottema, and Rosenbohm (11) as being due to the presence of iron in their samples, and concluded that the transition temperature is 640°C in iron-free cerium, with probably several transitions between 600°C and the melting point.

Ahmann (28) determined the melting point of cerium at 793±5°C with a solid transformation at 703±10°C. Spedding and Daane (8) later reported the melting point as 804°C and the transformation temperature as 754°C.

Herrmann's electrical resistivity measurements on cerium (4, p.120) detected a sharp increase in resistivity at 726° - 733°C, the increase being some 8.5 per cent of the total resistivity at that temperature.

A magnetic transformation, appearing as an 8 per cent decrease in the susceptibility on warming, was found by Gaume-Mahn (29) between 670°C and 710°C. Her cerium sample contained only 0.0005 per cent iron and 0.4 per cent silicon.

The addition of magnesium was seen to lower the transition temperature and decrease the effect of the transformation on the susceptibility.

Praseodymium

The crystal structure of praseodymium at room temperature was found to be hexagonal close-packed by Rossi (30, 31) and by James, Legvold, and Spedding (22), although the last publication reported some face-centered praseodymium as well. Klemm and Bommer (32) found the structure to be face-centered cubic, but later (33), with more pure material, reported only hexagonal close-packed. They noted some discrepancies existing in their diffraction pattern, however, and suggested that these might be removed by indexing the lines on the basis of a c_o lattice parameter double to that used. Herrmann (4, p. 47) recently verified this hexagonal form with the double c_o dimension to be the stable room temperature form.

There have been, to the author's knowledge, no solid phase transitions reported for praseodymium in the low temperature region, although Parkinson, Simon, and Spedding (24) did report an unexplained slight dip in the atomic heat at about -175°C.

The only previous dilatometric work on praseodymium was by Barson, Legvold, and Spedding (13), and was in the region below room temperature. A slight anomalous increase in the coefficient of expansion below about -75°C was noted, and the room temperature value given as 5.4×10^{-6} °C^{-1}.

In the high temperature region, a thermal arrest, apparently due to a phase transition, was reported by Spedding and Daane (8) at 798°C. This was in addition to the melting point as found at 935°C. Johnson and others (34) employed their vapor pressure apparatus to perform what was essentially a thermal analysis of praseodymium, and determined the melting point to be 919°C. Herrmann's electrical resistivity measurements (4, p.120) showed a sharp increase in the resistivity by 5.7 per cent at 789° - 795°C, corresponding to the high temperature solid transition.

Earlier magnetic susceptibility measurements by La Blanchetais (35) showed that a plot of the reciprocal susceptibility as a function of the temperature did not quite obey the linear relationship predicted by the Curie-Weiss law, but curved smoothly away below such a line above 225°C. Unfortunately, these measurements were carried no higher than 797°C, at which temperature the metal reacted slightly with the fused silica tube in which it was contained. No evidence of a phase transition at high temperatures was mentioned.

Neodymium

The room temperature form of neodymium was reported by Quill (36), Klemm and Bommer (32), and James, Legvold, and Spedding (22) to be hexagonal close-packed. In a later paper, reporting on more pure metal, Klemm and Bommer (33) suggested, as they did for praseodymium, that some few lines required a doubled c_o lattice parameter in order to be

explained. Ellinger (37), Behrendt (38), and Herrmann (4, p47) have all confirmed this suggestion in independent work.

The high temperature work of Jaeger, Bottema, and Rosenbohm (11) included measurements of electrical resistivity, specific heat, and thermal expansion. Their sample, however, was extremely inhomogeneous, showing large internal thermoelectric effects. Several anomalies and large hysteresis were found, but the authors believed that a transition from hexagonal close-packed to face-centered cubic took place at about 508°C and that a second transition took place at about 720°C.

A dilatometric study of neodymium metal by Trombe and Foex (39) disclosed an anomaly at 600° - 650°C which they associated with the hexagonal-cubic transformation mentioned by Jaeger, Bottema, and Rosenbohm. Values given for the expansion coefficient were 6.6×10^{-6} °C^{-1} between -195°C and 0°C, 7.4×10^{-6} °C^{-1} between 0°C and 200°C, and 7.8×10^{-6} °C^{-1} between 200°C and 400°C. Dilatometric work by Barson, Legvold, and Spedding (13) indicated no transitions in the low temperature region, and gave a room temperature expansion coefficient of 7.1×10^{-6} °C^{-1}.

The melting point of neodymium was found by Ahmann (28) to be 820±10°C, but rather large amounts of impurity were present in the form of 1 per cent magnesium and 0.5 per cent calcium. No solid phase transformation was detected below the melting point.

Spedding and Daane (8) reported the melting point to be 1024°C and found a transformation at 868°C as well. Thermal analysis by Johnson and others (34), in connection with vapor pressure studies, were in excellent agreement, indicating a melting point of 1019±2°C and a solid state transition temperature of 869±2°C.

High temperature electrical resistivity measurements by Herrmann (4, p.120) also indicated a transformation at 861° - 863°C. No other transitions were found at lower temperatures.

High temperature magnetic susceptibility measurements by Bates and others (40) showed no evidence of transitions from room temperature to 725°C, although the reciprocal susceptibility was found to be lower than the values predicted by the Curie-Weiss law from about 225°C upward.

Gadolinium

The crystal structure of gadolinium has been studied by Klemm and Bommer (32), Banister, Legvold, and Spedding (41), and Herrmann (4, p.63), all of whom found it to be hexagonal close-packed at room temperature. The data of Banister, Legvold, and Spedding showed, in addition, that in studies made down to -235°C this structure remained the stable form.

Probably the most interesting of the physical properties of gadolinium is its ferromagnetism, the Curie point being at about 16°C. This phenomenon was discovered by Urbain, Weiss, and Trombe (42) and later verified by Klemm and Bommer (32) and Elliott, Legvold, and Spedding (43). A

corresponding anomaly in the electrical resistivity near this point was found by Legvold, Spedding, Barson, and Elliott (44). Griffel, Skochdopole, and Spedding (45) found that a sharp peak in the atomic heat curve also occurred in the region of the Curie point, the entropy of magnetic order-disorder being slightly less than the R ln 8 calculated for a spin of 7/2.

A dilatometric study of gadolinium by Trombe and Foex (46) disclosed a sharp bend in the expansion curve at about the Curie point. For about 150°C below the Curie point, these investigators reported practically no expansion at all with changing temperature, that is, a zero coefficient of expansion. Above the Curie point, the coefficient was reported as considerably greater, near to those of other rare earth metals. A slight anomaly, with hysteresis, occurred at 100°C to 200°C. Banister's X-ray crystallographic study below room temperature (41) indicated that the a_o axis decreased normally with decreasing temperature below 50°C, but that the c_o axis increased. From the relative magnitudes of these effects, Banister was able to estimate the expansion coefficient for a bulk specimen as roughly 1×10^{-6} °C^{-1} below room temperature.

Using a rolled sample of gadolinium metal, Barson, Legvold, and Spedding (13) found the coefficient in this region to be slightly decreased from the room temperature value, but still no lower than about 5×10^{-6} °C^{-1}. In view of Banister's findings on the anisotropy of this metal, it was believed

that the rolling of the sample had produced a preferential orientation of the crystallites in the rod. This would explain, at least qualitatively, the differing results.

Other than the dilatometric work of Trombe and Foex, there has been practically no high temperature work on gadolinium. The melting point is known as approximately 1350°C from the work of Spedding and Daane (8), who recorded the temperature indicated by an optical pyrometer when the sample was observed to flow. Other than this, no high temperature anomaly has been reported.

Terbium

There has been but little work done on terbium metal, doubtless due to its scarcity in pure form.

Both Klemm and Bommer (32) and Herrmann (4, p.63) reported the room temperature crystal structure to be hexagonal close-packed. Klemm and Bommer, in the same article, reported the magnetic susceptibility to follow the Curie-Weiss law in the region immediately below room temperature, with a paramagnetic Curie temperature of about -70°C. They did not actually find the metal to become ferromagnetic, however, at temperatures as low as -175°C.

Recent unpublished work by Thoburn and others (47) seemed to indicate true ferromagnetism below about -40°C. The sample was impure and highly anisotropic, however, probably consisting of large grains, and this result is still somewhat tentative.

The melting point of terbium was reported by Spedding and Daane (8) as approximately 1400° - 1500°C.

Dysprosium

The crystal structure of dysprosium at room temperature was found to be hexagonal close-packed by Klemm and Bommer (32), Herrmann (4, p.63), and Banister, Legvold, and Spedding (41). The last authors reported this structure to be maintained as low as -235°C.

The interesting region for this metal is that below the range covered in the present work. At low temperatures this metal has what is apparently an antiferromagnetic state below -97°C and a truly ferromagnetic state below -180°C (48, 49).

The dilatometric study of dysprosium by Trombe and Foex (50) disclosed a plateau, or region of zero expansion, immediately below the temperature of the higher magnetic anomaly at about -97°C. Above this temperature, the expansion was perfectly smooth and gave no evidence of other transformations up to 300°C. The room temperature coefficient of expansion was about 8×10^{-6} °C^{-1}. Expansion measurements by Barson, Legvold, and Spedding (13) were in good agreement with the findings of Trombe and Foex in that region. Banister's X-ray analysis (41) showed that below about -100°C the c_o axis expanded with decreasing temperature, while the a_o axis contracted normally. From the values of the expansion of these axes, he estimated the macroscopic thermal expansion

of a bulk sample to be about 9×10^{-6} °C^{-1} above the magnetic anomaly and almost zero below.

The measurement of magnetic susceptibility was extended into the high temperature region as well by Trombe (51), who found the Curie-Weiss law obeyed up to a temperature above 450°C, with no indication of any high temperature anomalies.

The melting point of dysprosium is approximately 1500°C, as determined by Spedding and Daane (8).

Erbium

The only crystal structure reported for erbium is also hexagonal close-packed. This was found by McLennan and Monkman (52), Klemm and Bommer (32), Banister, Legvold, and Spedding (41), and Herrmann (4, p.63).

Erbium, like dysprosium, has a rather complex magnetic behaviour at low temperatures, becoming ferromagnetic below about -250°C, and probably antiferromagnetic between that temperature and about -195°C (53, 54). Anomalies of specific heat (55) and electrical resistivity (44) are associated with these magnetic transitions.

A dilatometric study of erbium by Barson, Legvold, and Spedding (13) covered the range from -175°C to room temperature. No anomalies were found in that region, and the room temperature coefficient of expansion was reported to be 9×10^{-6} °C^{-1}. The X-ray analysis of erbium by Banister, Legvold, and Spedding (41) once more showed an anisotropy below the Curie point similar to that in gadolinium.

Estimates of the expansion of a bulk sample of erbium from these data gave 10 x 10^{-6} $°C^{-1}$ above -175°C and about zero below that temperature.

Ytterbium

Ytterbium, unlike its neighbors in the periodic table, was found by Klemm and Bommer (32) and by Herrmann (4, p.53) to crystallize in the face-centered cubic form at room temperature. Bommer (56) pointed out the striking increase in atomic radius of this metal, as well as europium and to some extent samarium, over the others in the rare earth series. These elements tend to have radii corresponding to divalent metals, a valency state which they often assume in compound formation.

Bridgman (57), in performing high pressure measurements, found an extreme effect upon the electrical resistivity of this metal, that property increasing rapidly with pressure to a maximum some thirteen times its normal value at a pressure of 50,000 kg/cm^2. Above about 60,000 kg/cm^2, however, the resistivity suddenly decreased to a value less than its normal one, where it remained relatively constant under further increases of pressure. The compressibility measurements were not made to pressures high enough to include the anomalous range, but indicated a compressibility some two to three times as great as that of other members of the rare earth series.

A thermal analysis of this metal by Spedding and Daane (8) determined the melting point to be at 824°C, and also disclosed a second thermal arrest at 798°C.

APPARATUS

A schematic diagram of the equipment used in the present investigation is shown in Figure 1. The apparatus resembled a fused-quartz tube and dial-indicator dilatometer in which the dial-indicator was replaced by an interferometer for increased sensitivity. Provision was made for heating the sample under an inert atmosphere of purified helium gas, and the progress of each experimental run was recorded continuously on an automatic strip chart recorder. A detailed description of the various components and their operation follows.

Description of Components

Sample Holder and Interferometer

The sample holder and interferometer, which together made up the working parts of the dilatometer, are shown in Figure 2.

The sample holder consisted of a fused silica tube with a sealed conical bottom on which the metal sample rested. The sample was in the form of a rod some 5cm long and 0.6cm in diameter. Resting in turn upon the sample was a fused silica rod topped by an aluminum adaptor for supporting the lower optical flat. The upper optical flat, as shown in the figure, was supported by three steel adjusting screws which were essentially fixed rigidly to the silica tube. Thus, any change in length of the sample appeared as a motion of

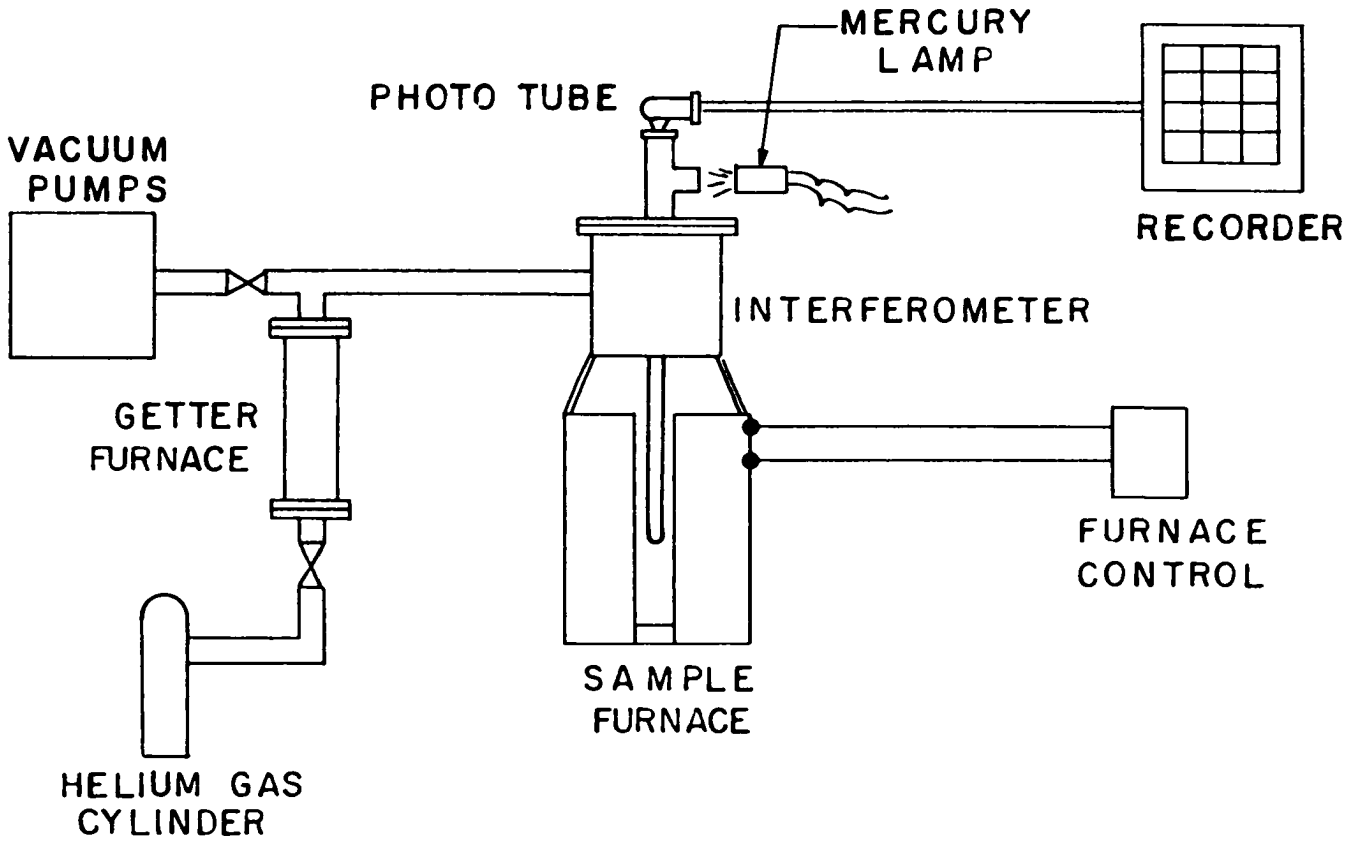

Figure 1. Schematic Diagram of Apparatus

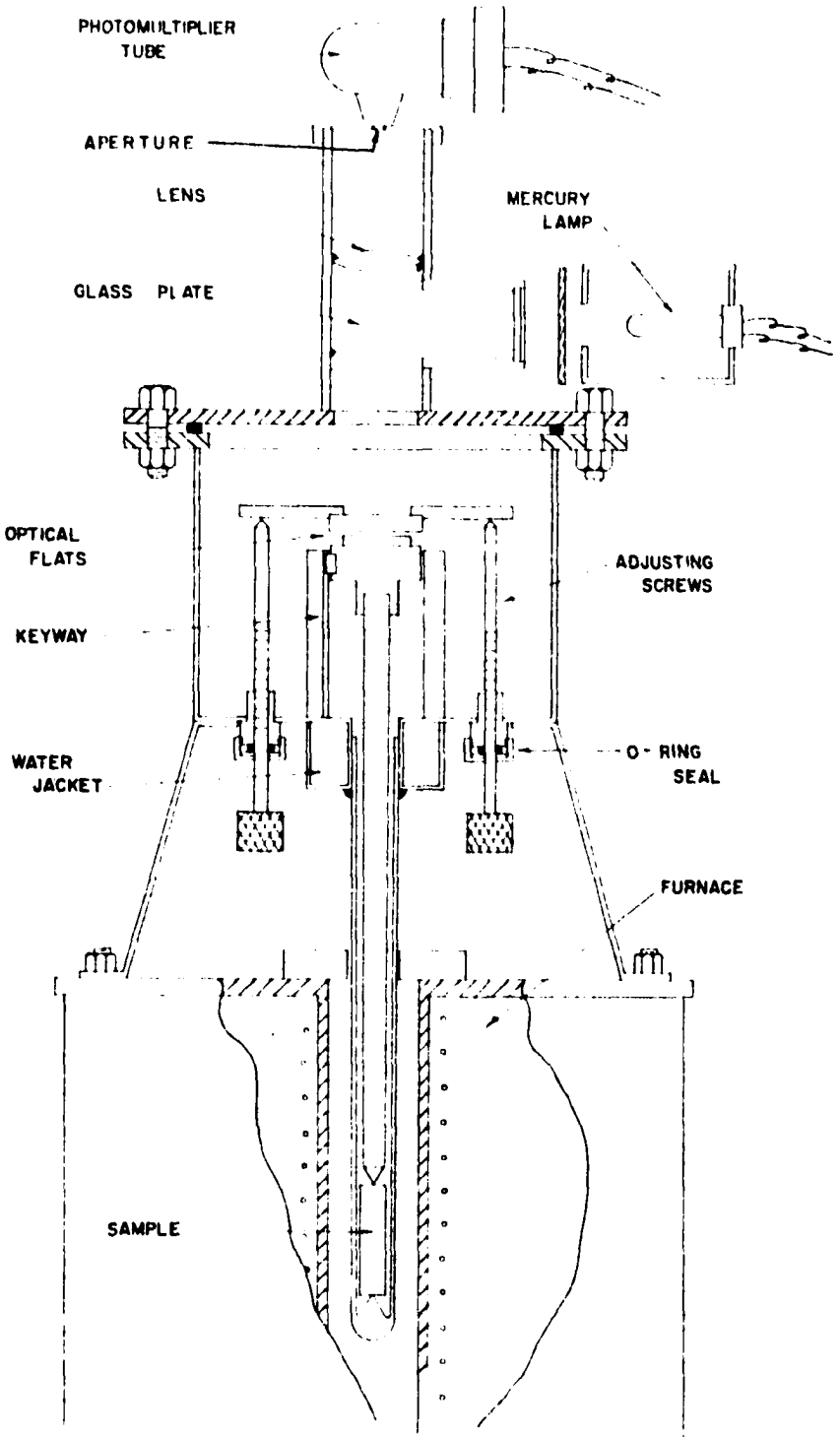

Figure 2. Detail of Sample Holder and Interferometer

the fused silica rod relative to the surrounding tube and was transmitted as a relative motion of the two optical flats.

In order to measure quantitatively the relative motion, the optical flats were illuminated with monochromatic light and adjusted nearly to parallelism. Small windows permitted the operator to see the separation of the flats as an aid in their adjustment. When they were properly adjusted, there appeared slightly curved interference fringes which moved one way or the other, depending upon whether the sample expanded or contracted. The analysis is identical to that of localized fringes produced in the Michelson interferometer (see Jenkins and White (58) for example), and indicates that one fringe will pass some fixed point whenever the distance between the optical flats changes by one-half the wave length of the monochromatic light used. In the present case, the light source employed was a mercury arc lamp with a narrow band filter which passed the mercury green line of wavelength 5460.7 A.

It was, of course, important to prevent heating of the interferometer as the furnace temperature was increased. Convection within the sample holder was minimized by a close fit between the silica rod and tube; convection outside of the sample holder was minimized by a tight plug in the bottom of the furnace and a loosely fitting one at its top. A water jacket at the top of the silica tube also helped to cool the interferometer, as well as to prevent a wax seal

at this point from softening. With this arrangement, the interferometer was kept always at room temperature and the sample always at the temperature of the center of the furnace. The temperature gradient, then, occurred entirely along the silica rod and tube. Since these were of the same material, their expansions just canceled, and the motion transmitted to the optical flats was due only to the expansion of the sample itself, less the expansion of an equal length of silica corresponding to the tube around the sample. Since this part of the tube was always at the same temperature as the sample, and since the expansion of fused silica is well known and quite small, a correction for this could readily be made.

It might be pointed out that the use of steel adjusting screws to support the upper optical flat, and an aluminum adaptor to support the lower one, was a deliberate choice of materials to minimize the effect of changes of room temperature. Since the expansion of aluminum is appreciably larger than that of steel, the lengths of these two materials could be adjusted to compensate each other, assuming only that they remained at a common temperature. Since these were all enclosed in the same helium atmosphere, this assumption was considered to be a good one; it seemed to be, in fact, when the room temperature was deliberately changed over a small range.

A small key and keyway, indicated on the diagram, prevented the lower optical flat from rotating. A close but

free fit of the adaptor supporting the lower flat prevented excessive wobbling or tilting of this part of the interferometer. To insure a stable positioning of the upper optical flat, the three adjusting screws were seated respectively in a V-groove, a conical hole, and a flat surface, all machined in the holder for the upper optical flat. With these precautions, the apparatus was stable to all but rather severe jarring of the equipment, and was not disturbed by the usual vibrations in the building.

Inert Atmosphere

Since the rare earth metals are extremely reactive, particularly at elevated temperatures, it was necessary to maintain either a vacuum or an inert atmosphere about them at all times during the run. The use of a helium atmosphere, rather than a vacuum, was chosen partly to maintain thermal equilibrium between the fused silica rod and tube along their lengths, and partly to minimize vaporization of the several rare earth samples whose volatilities are high at elevated temperatures.

The scheme for purifying the helium gas used is indicated in the diagram of equipment previously shown in Figure 1. With the sample furnace still cold, the equipment was evacuated with the mechanical pump, flushed with helium gas, and evacuated to a high degree with an oil diffusion pump. The getter furnace, packed with alternate layers of pyrex wool and turnings of a 90 per cent calcium - 10 per cent magnesium

alloy, was then heated to 500°C to outgas. When a good vacuum was obtained once more, the temperature of the furnace was reduced to 400°C where it remained during the entire run. The system was then closed off from the pumps and filled with helium gas, which flowed in over the hot getter. With the helium gas at approximately atmospheric pressure, the system, including the getter furnace, was sealed off. With such an isolated system, the gas density remained constant at all times, so that even if the temperature and pressure varied slightly, the refractive index of the gas was unchanged. Hence, no error was introduced in the results due to changes in the wavelength of the monochromatic light.

A further precaution, necessary to protect both sample and equipment, was to prevent the metal from reacting with the fused silica, a reaction which proceeds very readily at high temperatures. Thin tantalum foil was wrapped around the sample and discs of this foil fastened to each of its ends, thus preventing any direct contact of the rare earth metal with the fused silica.

Thermometer

To measure the temperature of the sample during the runs, a chromel-alumel thermocouple was employed, using a calibration from the manufacturer. Calibration points were supplied at 500°F, 1000°F, 1600°F, and 2000°F, or over an interval up to almost 1100°C. In the range covered by the present investigation, up to about 950°C, the deviation of the thermo-

couple readings from the standard tables at the calibration points was less than 40 μv, or about a degree.

The thermocouple was secured to the outside of the fused silica sample holder tube at a point near the center of the sample length. This placement outside of the sample holder was made necessary first because chromel-alumel thermocouples are calibrated to be used in oxidizing atmospheres, and second because vapor from the more volatile rare earth metals may react with the thermocouple materials very readily at high temperatures. In order that the thermocouple might more nearly read the true temperature of the sample at all times, both the thermocouple and the sample holder were wrapped together with a small amount of "Refrasil" quartz fiber insulation. It is believed that this permitted the thermocouple to "see" the sample more readily than the furnace.

In order to check the difference between the true sample temperature and the temperature indicated by the thermocouple placed outside of the sample holder as indicated above, a preliminary experiment was performed. A small length of steel tubing was inserted in place of the sample, and a second thermocouple junction placed inside of this tubing. This thermocouple was connected in opposition to the outer one as a difference thermocouple, and the furnace was warmed and cooled at rates identical to those employed in gathering the data on the rare earths. This permitted the direct

reading of the correction required at any point in the course of a run. Furthermore, by raising and lowering the inner thermocouple slightly, one could estimate the magnitude of the temperature gradient existing along the sample.

It was determined that the maximum temperature difference between any two points on the sample was probably no more than 4°C, and this much only at the very highest temperatures attained during the runs. Over most of the range it was less than 2°C.

The difference between the mean sample temperature, as estimated from the temperature gradients measured above, and the thermocouple reading outside of the silica tube was found to be of the same order of magnitude. It varied smoothly and almost linearly from zero at room temperature to about 4°C at the highest temperature reached. In using the thermocouple, a correction was made for both this error due to the thermocouple placement and for the calibration as furnished by the manufacturer. It is estimated that the temperatures so indicated represented the true sample temperature to about ± 2°C, and, since the corrections varied smoothly with temperature, that temperature differences over a limited range could be determined considerably more accurately than this.

Recorder System

In order to record the results of the experimental work continuously, both the thermocouple reading and the motion of the interference fringes had to be recorded. The

instrument used in this work was a Bristol "Dynamaster" two-pen recording potentiometer. Full-scale deflection for each pen was 2 mv, a span which could be traversed by either pen in 2 seconds. The instrument automatically standardized itself against a standard voltage reference cell at 15-minute intervals, and the manufacturer claimed an accuracy of 0.1 per cent of the full scale reading, although this last seemed rather doubtful to the author.

A full-scale reading of 2 mv was desirable in order to give sufficient sensitivity in the thermocouple readings. Since the thermocouple readings went as high as 40 mv, however, some revision in the circuitry was obviously necessary.

The method used to expand the range of the recorder was a modification of the method of Chiotti (59), and is shown in Figure 3. It consisted in part of a regulated voltage supply in series with twenty-four 10-ohm precision resistors and a helipot with which to control the voltage drop across these resistors. This voltage drop was monitored manually with a Rubicon B precision potentiometer and maintained at a total voltage of 47.1 mv, or 1.96 mv across each 10-ohm resistor.

A microswitch on the upper end of the recorder span was closed by the pen as it reached the upper limit of the scale. This microswitch actuated a stepping switch that placed one of the 10-ohm resistors into the thermocouple circuit with its 1.96 mv opposed to the thermocouple voltage. This almost

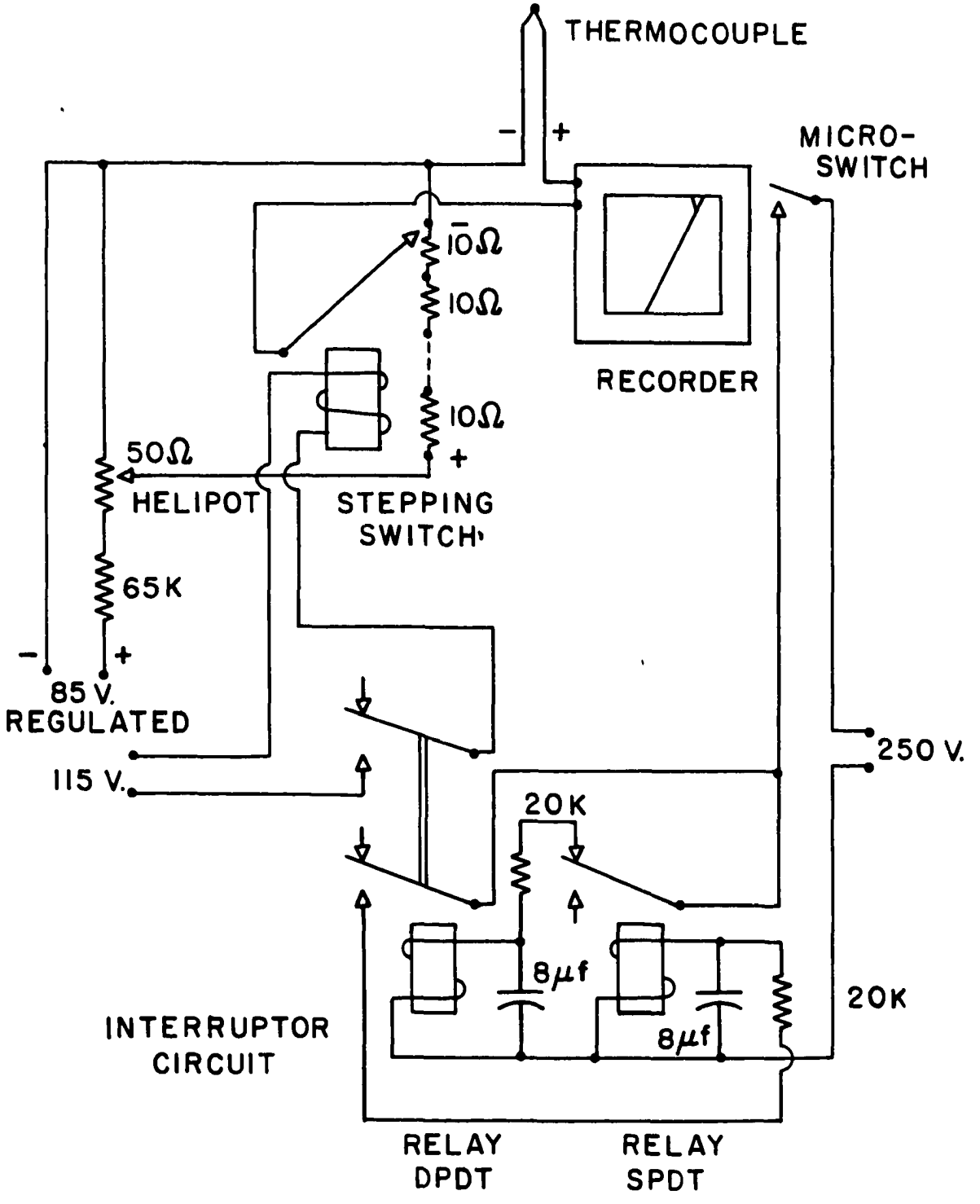

Figure 3. Thermocouple Circuit Diagram

entirely balanced out the thermocouple voltage, reducing the net voltage applied to the instrument almost to zero and starting the pen over again at the bottom of the span. As the pen again advanced to the top of the scale, a second voltage was switched in automatically, and so on.

In the event that the stepping switch might be more than one step away from the correct setting, such as in turning on the equipment, it would be necessary to pulse the stepping switch repeatedly in order to bring it to the proper position. Hence, it was necessary to install an interruptor such as is shown in the figure, into the microswitch circuit. The values of the condensers and resistors were such that the stepping switch was pulsed at approximately one-second intervals until the proper setting was reached and the recorder pen returned to the bottom or middle of the scale.

Actually, only half of the circuit is shown in the figure, since an identical circuit was used with a microswitch at the bottom of the recorder scale to advance the stepping switch in the opposite direction. The instrument could then be used in either the warming or the cooling direction. A series of pilot lights on the control panel indicated to the operator the position of the stepping switch at any time, so that the actual thermocouple voltage could be calculated from the recorder reading at that time.

The second pen of the two-pen recorder was used to indicate the passage of interference fringes caused by changes

in length of the sample. In Figure 2, showing the details of the interferometer, a lens was indicated above the optical flats. This lens focused an image of the interference fringes onto the plane of the cover of this equipment, where part of the light reached a photomultiplier tube through a small aperture. Since the aperture was small compared to the width of the fringes, the photomultiplier tube "saw" sinusoidal variations in light intensity as the fringes moved past. A somewhat similar scheme for counting fringes has been used in the Fizeau-Pulfrich dilatometer by Work (60), Peck and Obetz (61), and others.

Figure 4 shows the circuit diagram for the photomultiplier tube. The variation of light intensity from the fringes appeared as a variation in plate current of the tube and, hence, as a variation of voltage across the 1 megohm resistor in the plate circuit. Such a variation in voltage was suitable to apply to the recorder. It was convenient, however, to use the 100 K potentiometer indicated in the figure as a voltage divider to control the amplitude of the signal. The regulated voltage supply and potentiometer made it possible to buck out much of the d.c. part of the signal and center the sinusoidal a.c. component on the recorder chart. Each cycle of this a.c. component represented the passage of one interference fringe, or a change in separation of the optical flats of 2730.4 A, a half-wavelength of the mercury green line used to illuminate the flats.

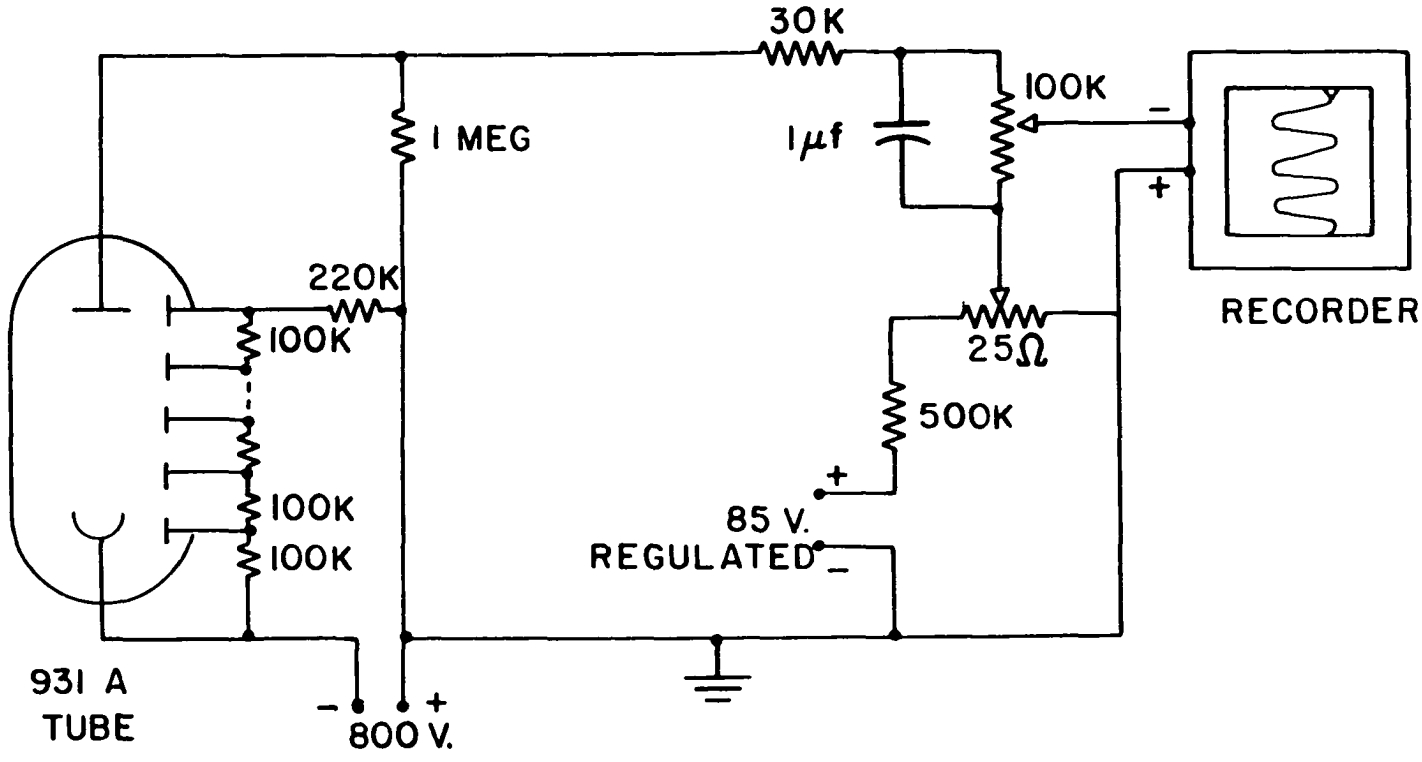

Figure 4. Photomultiplier Tube Circuit Diagram

To illustrate the type of record obtained, a sample strip of chart, reduced to about one-half size, is shown in Figure 5. This particular section of chart was actually taken from one of the lanthanum runs in this investigation. It is especially interesting since it includes a transition in which the sample, originally expanding with increasing temperature, changed direction and contracted sharply over a short range, then reversed once more and expanded in a normal fashion. The points of reversal are clearly evident toward both ends of the section of chart shown. Thus, while the direction of motion of the optical flats is not obvious from the fringe pattern at any time, reversals are usually readily apparent. In regions of transition, or at any time of doubt, the operator can remove the photomultiplier tube from the apparatus, examine the fringes visually, and infer the direction of motion of the optical flats from the observed fringe motion. The optical flats being very nearly parallel, the fringes appear curved or actually circular. If the fringe motion is one of expanding circles, this indicates that the separation of the optical flats is increasing, or that the sample is contracting. Conversely, contracting circular fringes indicate that the sample is expanding.

Furnace Control

With the above provisions for recording both temperature and fringe count continuously, there remained only the need for a mechanical temperature control to make the dilatometer completely automatic.

Figure 5. Sample of Strip Chart Record

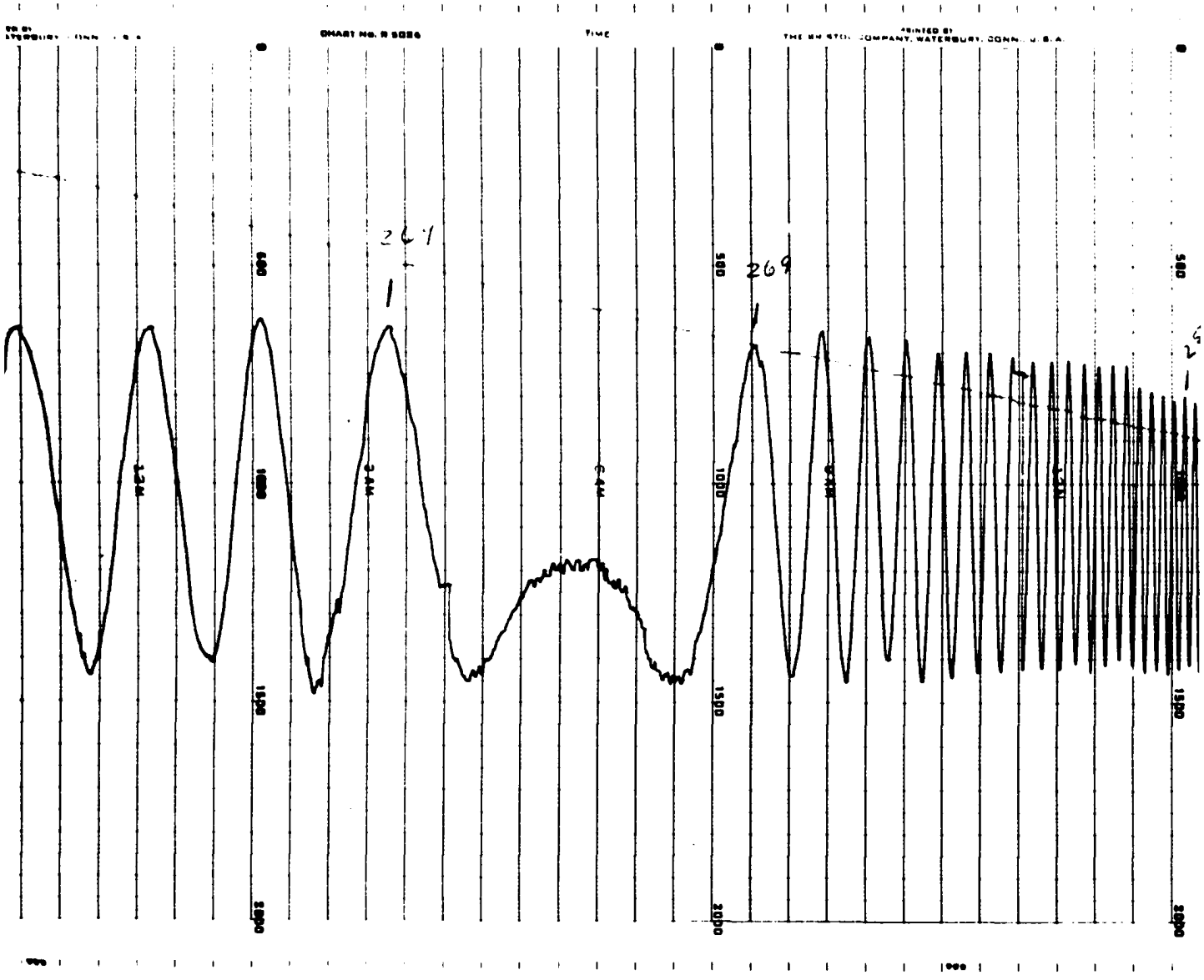
CHART No. R 5086
TIME
261
269
1.2M
2.4M
6.4M
9.6M
500
1000
1500
2000

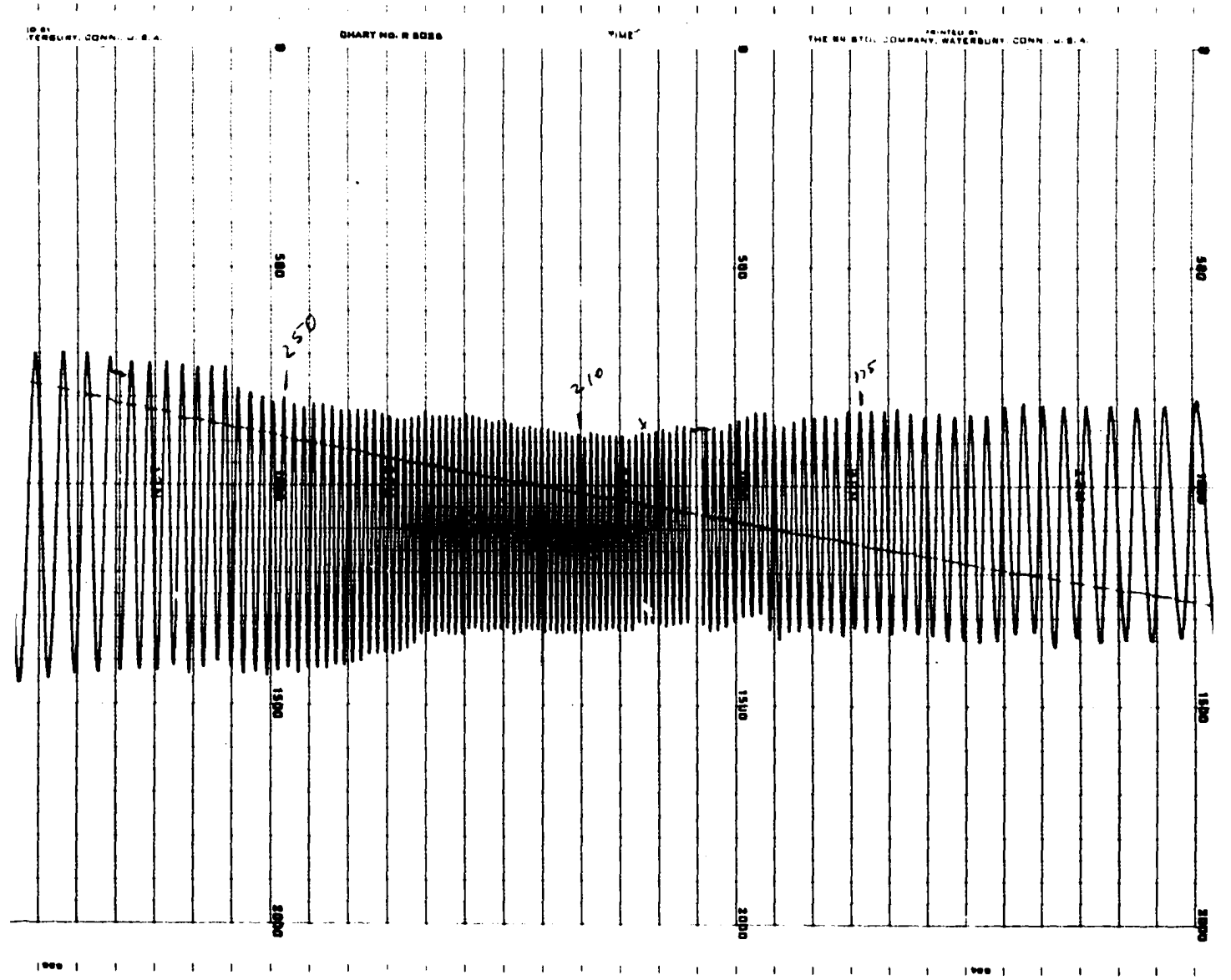
CHART NO. R 5026
TIME
250
210
175
500
1000
1500
2000

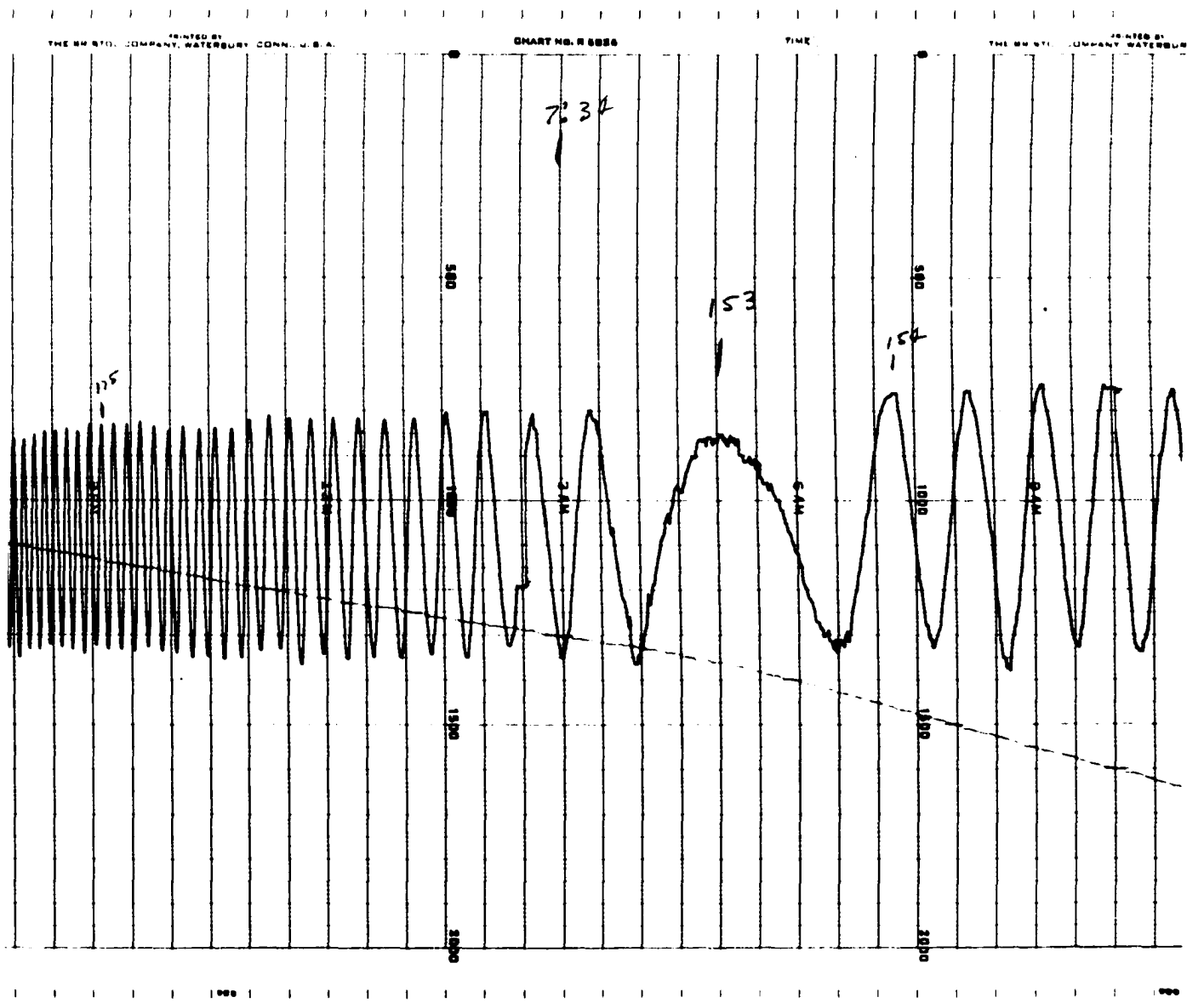
CHART NO. R 6826
TIME
7:34
153
154
175
500
1000
1500
2000
3.4M
6.4M
9.4M

Slow rates of heating and cooling were essential to insure an approximation of equilibrium conditions. Preliminary work showed that the most favorable method seemed to be that of advancing the furnace setting in discrete steps and allowing time between for the sample, thermocouple, and sample holder to approach equilibrium.

The device used to achieve this end was simply a motor-driven powerstat, the motor being turned on for a short time once in each hour by a clockwork mechanism. The amount of the advance each hour was slightly over a volt, or enough to increase the furnace temperature by about 25°C to 30°C in that time. Readings were taken from the chart record at the end of each hour, just prior to a new change in furnace setting, when the temperature of the furnace was changing very slowly. The time axis on the chart made it possible to determine the proper points for taking the data without giving the equipment constant attention throughout the run.

The motor used to drive the powerstat was a reversing type, geared down to a very slow rate of rotation. When the maximum desired temperatures had been attained, the operator had only to reverse the direction of the motor for the furnace to be cooled in discrete steps at much the same rate as it had warmed.

Evaluation of Performance

Trial Measurement of Copper

In order to test the operation of the dilatometer, a sample of 99.999 per cent copper was run in the equipment in exactly the manner of operation used with the rare earth metals. The sample was of comparable size and was protected by tantalum foil, even though this was not strictly necessary in the case of a metal such as copper.

The thermal expansion of this sample, reduced to unit length, is shown in Figure 6. The slight correction for the length of fused silica surrounding the sample has been made. In this calculation, and in all subsequent calculations on the rare earth metals, the expansion data for silica were obtained from the results of Saunders (62) at the National Bureau of Standards.

It may be noticed that the slope of the curve of Figure 6 is $\frac{1}{L_o}\frac{dL}{dt}$ which is exactly the coefficient of expansion of the metal. Hence, to determine the expansion coefficient of the copper, and in fact of the rare earth metals as well in analyzing those results, one has only to plot the expansion curve to a large scale and differentiate it graphically.

The data for copper, as here determined, were so treated to give the expansion coefficient as a function of temperature between room temperature and about 900°C. In order to compare these results with those of other investigators, the present values and the data reported in the literature

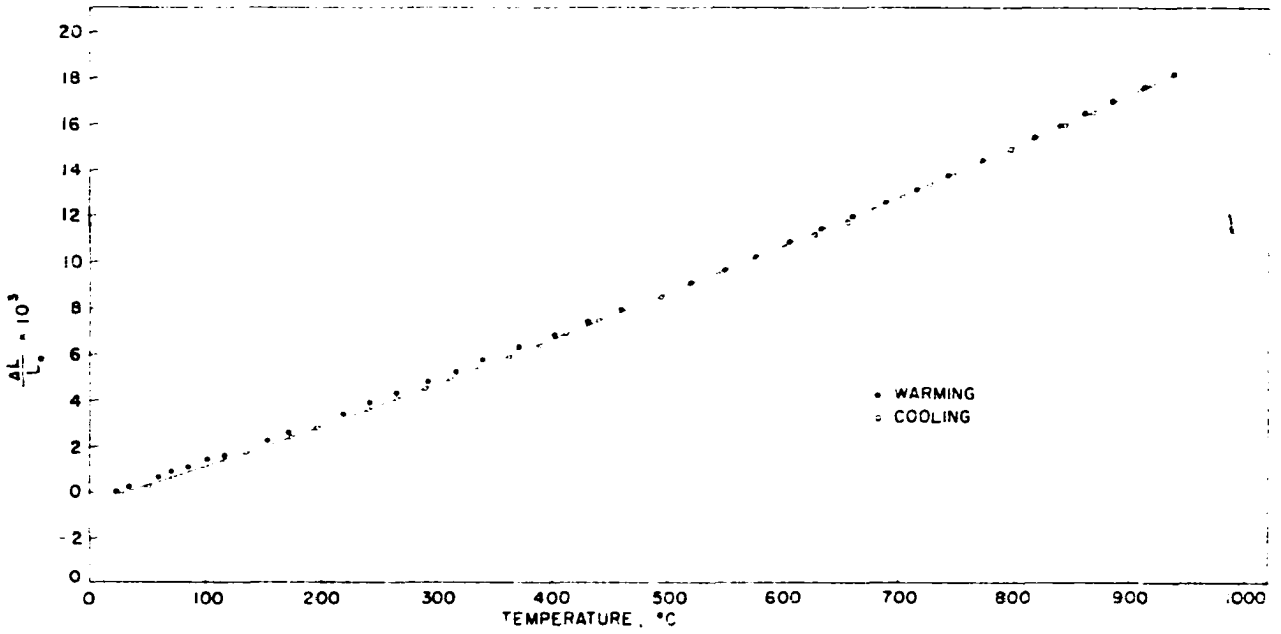

Figure 6. Thermal Expansion of Copper

are plotted together in Figure 7. The scale is deliberately large in order to exaggerate the differences and the scattering of points. It is seen that the results of the present investigation are in satisfactory agreement with the values reported by Esser and Eusterbrock (63), Dittenberger and Gehrcke (64), Nix and MacNair (65), and Henning (66), but are in rather poor agreement with the results of Rosenbohn (67), Uffelman (68), and Eucken (69). It may be noted that the warming run of the present work gave results which were apparently slightly low over part of the range. It was found in later work that this was generally true for the rare earths as well, usually to a much greater degree, but that following the first warming run the results became reproducible. This was probably due to an annealing of the sample, or perhaps to a relaxation of slight strains in the thin tantalum discs on the ends of the sample. At any rate, the results of the first warming run were generally discarded in subsequent work.

In view of the rather large discrepancy among some of the results reported in the literature, even for a well-behaved metal such as copper, it is felt that the results of the present work on copper were sufficient to verify the accuracy of the equipment, at least to within the limits achieved by other investigators.

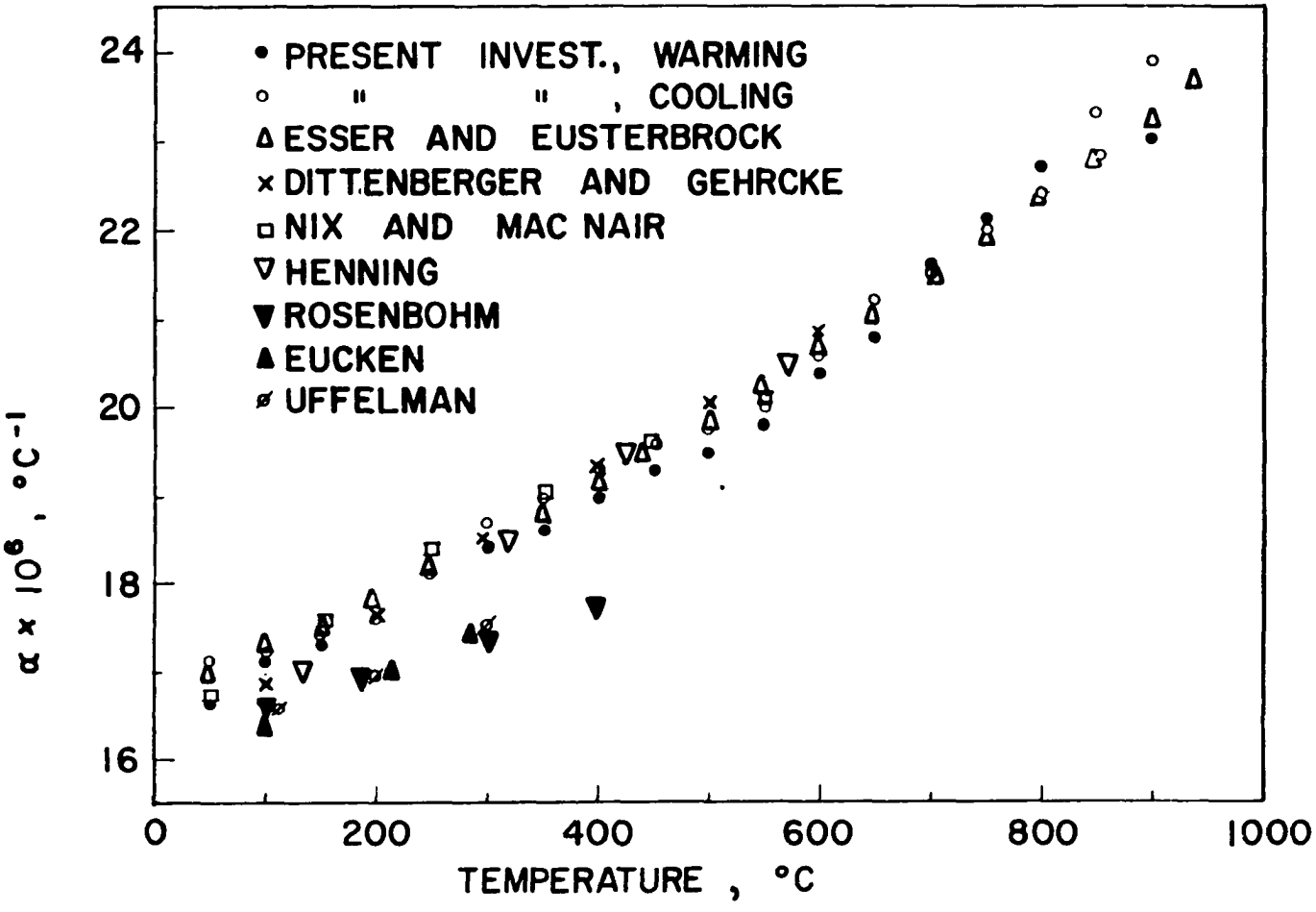

Figure 7. Expansion Coefficient of Copper

Estimate of Accuracy

It is difficult to estimate the accuracy of the instrument quantitatively, since many small effects which may introduce error are difficult to measure.

The calculations involved only the original length of the sample, the number of fringes which had passed, and the temperature. The sample length could be measured to much less than 0.1 per cent. A slight correction was made for the tantalum foil on the ends of the sample, even though the thickness of both discs together amounted to only about 0.1 per cent of the sample length. The number of fringes in any temperature interval could be read from the chart with an accuracy of about a tenth of a fringe or better if the count was marked at the peak of a fringe, these peaks being quite sharp. It is believed that a temperature interval of about 30°C could be measured to at least $\pm$ 0.3°C, and probably better, provided the operator monitored the calibration of the circuitry for expanding the scale of the recorder. In a temperature range of this size perhaps fifty fringes would be counted for a typical rare earth metal. Thus, one would be led to estimate that the coefficient of expansion could be determined to about one per cent or slightly more over a range of 30°C. This was about the span between readings under normal operating conditions.

Actually, the data were not this precise, as was indicated by the scattering of points about the curves and the

lack of reproducibility to this high degree. It seems likely, however, that the slightest amount of strain or binding in the moving parts of the equipment would be sufficient to exceed the stringent requirements for this amount of accuracy. It is possible that the amount of freedom required by the moving parts in order to minimize such binding was enough to permit a very slight tilting of one optical flat relative to the other. This would have the effect of changing the density of the interference fringes, that is, the distance between the maxima and minima, and would cause additional fringes to cross the field and be counted. It is also possible that the effect on the apparatus due to small changes in room temperature was not completely eliminated. All of these effects are probably quite small. Although it is difficult to estimate them quantitatively, they seem adequate to explain the failure to achieve the high precision indicated by the estimate of error involved in reading the instruments.

Since the data were not precise enough to calculate the coefficient directly within 1 per cent in these intervals, the expansion curve was differentiated graphically from a curve drawn through the points. Since the points did not deviate much from a smooth curve, as will be seen in the figures to be presented, it is believed that little error arose from the differentiation process itself.

In addition to the effects mentioned above, it seems likely that the expansion of the sample itself may actually

not be as smooth and regular as one would like to see in an ideal graph. This would particularly be suspected in the high temperature range, where diffusion, crystal growth, and the introduction of lattice defects may become appreciable.

In view of the results obtained with copper relative to the values reported in the literature, and judging from the degree of reproducibility and scatter of points in the subsequent runs on rare earth metals, it is the author's opinion that an accuracy of about $\pm$ 0.2 x 10^{-6} $^{\circ}C^{-1}$ in the values of the expansion coefficients reported is a reasonable claim. This is approximately a two per cent probable error in the coefficient of expansion, although it is believed that the total change in length of the sample over the entire run was measured with an accuracy of better than one per cent.

MATERIALS TESTED

Preparation

The separation of rare earths has long been a difficult problem, due to their close chemical similarity. The salts used to produce the metal samples for this investigation were separated and purified by the ion-exchange process described by Spedding and others (70, 71). To produce compact metallic samples, the fluorides of the various metals, with the exception of ytterbium, were bomb reduced with calcium metal. This technique, which gives excellent yields, was devised by Spedding and Daane (72, 73). Following the reduction, the metals were vacuum cast to distill off the excess calcium remaining. In the case of ytterbium, it was found that calcium did not reduce the ion to the metallic state, so that another method had to be found. A successful reduction was performed by Daane, Dennison, and Spedding (74) by reacting metallic lanthanum with ytterbium oxide to yield metallic ytterbium, lanthanum oxide, and some excess lanthanum. Since the vapor pressure of ytterbium metal is considerably greater than that of lanthanum or its oxide, it was possible to distill off practically pure ytterbium metal from the resulting mixture.

Following the purification of these metals, they were recast into rods slightly larger than the size required, and then turned to shape in a lathe. The finished sample was in all cases a rod some 5cm long by 0.6cm in diameter. All casting of these metals, including the reduction and

purification processes, was done in tantalum crucibles, a material which does not react appreciably with the rare earth metals except at very high temperatures.

Purity

It is, of course, desirable to have samples of the highest possible purity in conducting any experimental measurements. However, this is often rather a difficult thing to attain with rare earth metals. Fortunately, as Nix and MacNair pointed out (65), a small amount of impurities plays a minor role in the thermal expansion of non-ferromagnetic metals, and even in the case of ferromagnetic metals the effect is small except in the region about the Curie point. In this range, however, the effect may be very large.

In the present investigation, small amounts of metal from the final castings were examined to find the impurity content of each sample. These were analyzed chemically for carbon and nitrogen, and also spectroscopically. The results of these analyses are reported below, except in the cases of cerium, gadolinium, and terbium. These analyses, unfortunately, were not completed at the time of writing and could not be included.

The gadolinium sample, however, was taken from the massive block of metal used for heat capacity measurements by Griffel, Skochdopole, and Spedding (45). These authors reported impurities as follows for the gadolinium: tantalum,

less than 0.3 per cent; calcium, less than 0.04 per cent, and silicon, iron, and magnesium all less than 0.01 per cent. No other rare earth metals were detected. Presumably the gadolinium sample used in the present work would have about the same analysis, with possibly some additional tantalum and nitrogen resulting from the recasting process. The overall sample purity was probably about 99.5 per cent or better. The cerium and terbium samples would probably have an impurity content comparable to the following analyses for the remaining samples.

The lanthanum sample was a particularly pure one, approximately 99.9 per cent pure. The analysis showed it to contain 175 parts per million (ppm) of carbon, 400 ppm of nitrogen, and 0.04 per cent of calcium. The following elements were not detected spectroscopically: aluminum, beryllium, selenium, tantalum, yttrium, and all other rare earth metals.

The praseodymium sample had an analysis showing it to contain 309 ppm of carbon and 470 ppm of nitrogen. Rather a high percentage of neodymium, about 0.2 per cent, was also found. In addition there was less than 0.1 per cent cerium, 0.03 per cent tantalum, 0.03 per cent silicon, 0.01 per cent lanthanum, and 0.006 per cent iron. By difference, the sample purity was about 99.5 per cent.

The neodymium sample was about 99.7 per cent pure, containing less than 0.08 per cent praseodymium, 0.06 per cent samarium, 0.01 per cent calcium, 0.025 per cent silicon,

0.05 per cent tantalum, and 0.006 per cent iron. The carbon content was reported as 175 ppm, and the nitrogen 600 ppm. Lanthanum and cerium were not detected.

A rather impure dysprosium sample was used in the present work, since the analysis indicated it to be only about 99.0 per cent. A high percentage of tantalum was present, about 0.5 per cent. Possibly it had been heated to too high a temperature at some time in its production while in a tantalum crucible. In addition it was contaminated with about 0.2 per cent of calcium, and no more than the following amounts of impurities: terbium, 0.1 per cent; holmium, 0.05 per cent; erbium, 0.02 per cent; iron, 0.005 per cent; and silicon, 0.02 per cent. Gadolinium was not detected, but 95 ppm of carbon and 30 ppm of nitrogen were.

A relatively pure sample of erbium was procured for this work, containing about 0.07 per cent calcium and 0.03 per cent iron. In addition there was no more than 0.005 per cent dysprosium, 0.01 per cent holmium, 0.04 per cent silicon, 0.002 per cent thulium, and 0.01 per cent ytterbium. The carbon content was 95 ppm and the nitrogen content was 30 ppm. The purity of the sample was thus about 99.8 per cent.

The ytterbium sample contained 645 ppm of carbon and 100 ppm of nitrogen. The largest metallic impurity was calcium, in the amount of 0.5 per cent. There was also present about 0.05 per cent each of iron and silicon, and less than 0.01 per cent erbium, 0.005 per cent lutetium, 0.03 per cent

tantalum, and 0.01 per cent thulium. A trace of copper also was detected, and the purity of the sample, by difference, was estimated as about 99.3 per cent.

RESULTS

Lanthanum

The expansion of lanthanum, as determined in the first trial, is shown in Figure 8. The most notable feature of this study was the transition at moderate temperatures with considerable hysteresis. This transformation corresponds to the hexagonal close-packed to face-centered cubic transition, the hexagonal form being stable at lower temperatures. It was centered at about 310°C in the warming direction and was fairly abrupt, going almost to completion within a range of 20°C. In the cooling direction, the transition occurred largely between 200°C and 240°C but was sluggish and incomplete, probably due to the lower temperature. The decrease in length accompanying this transformation was about 0.1 per cent of the total length, in the warming run, or, assuming an isotropic sample, about 0.3 per cent by volume. In the cooling direction, the volume change was only about half as great, indicating that some face-centered cubic lanthanum was probably still present at room temperature following the run.

The present results are in fairly good agreement with the work of Trombe and Foex (12) who found a hysteresis loop in the expansion curve between 150°C and 350°C. These investigators reported only a 0.19 per cent change in volume, however. It might also be recalled that Bridgman (14)

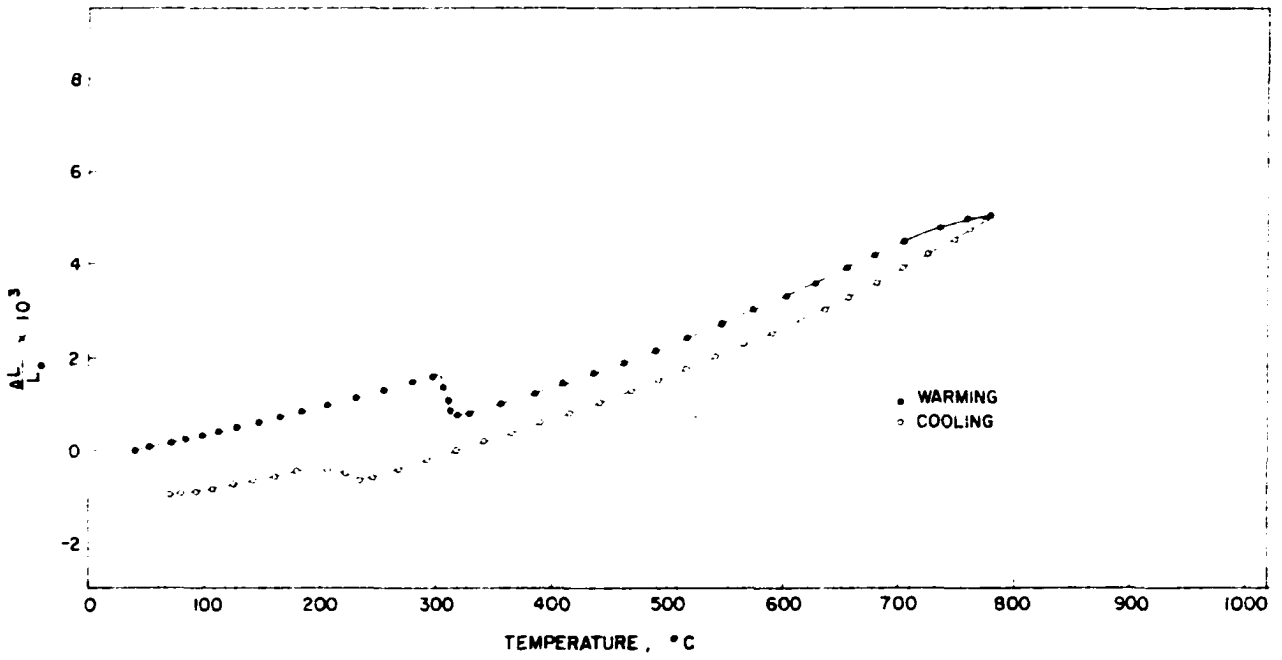

Figure 8. Thermal Expansion of Lanthanum, Run 1

detected an abrupt volume change of 0.26 per cent at high pressures, a value close enough to that found here to suggest that the transformations are the same in both cases.

A second unusual feature of the expansion curve as here measured was the softening at higher temperatures, the sample taking on a permanent decrease in length. In a second run on lanthanum, shown in Figure 9, the sample was warmed to a higher temperature than in the first run, with the result that the sample became so soft as to be deformed by the very small weight which it supported, that of the fused silica rod and lower optical flat. The temperature of this occurrence was still about 60°C below the reported melting point.

It was unfortunate that this effect made it impossible to take usable data through the anticipated high temperature transition as detected by electrical resistivity and thermal analyses.

It might be noticed that the lower temperature transformation in the second run was marked by a volume change of only about 0.2 per cent, considerably less than in the first run, and indicating once more that a mixture of more than one crystalline form was probably present.

The coefficient of expansion of lanthanum is shown in Figure 10. The room temperature value of about 4.8×10^{-6} $°C^{-1}$ is in good agreement with previous work done by Barson, Legvold, and Spedding (13), but is somewhat lower than the 5.8×10^{-6} $°C^{-1}$ reported by Trombe and Foex (12).

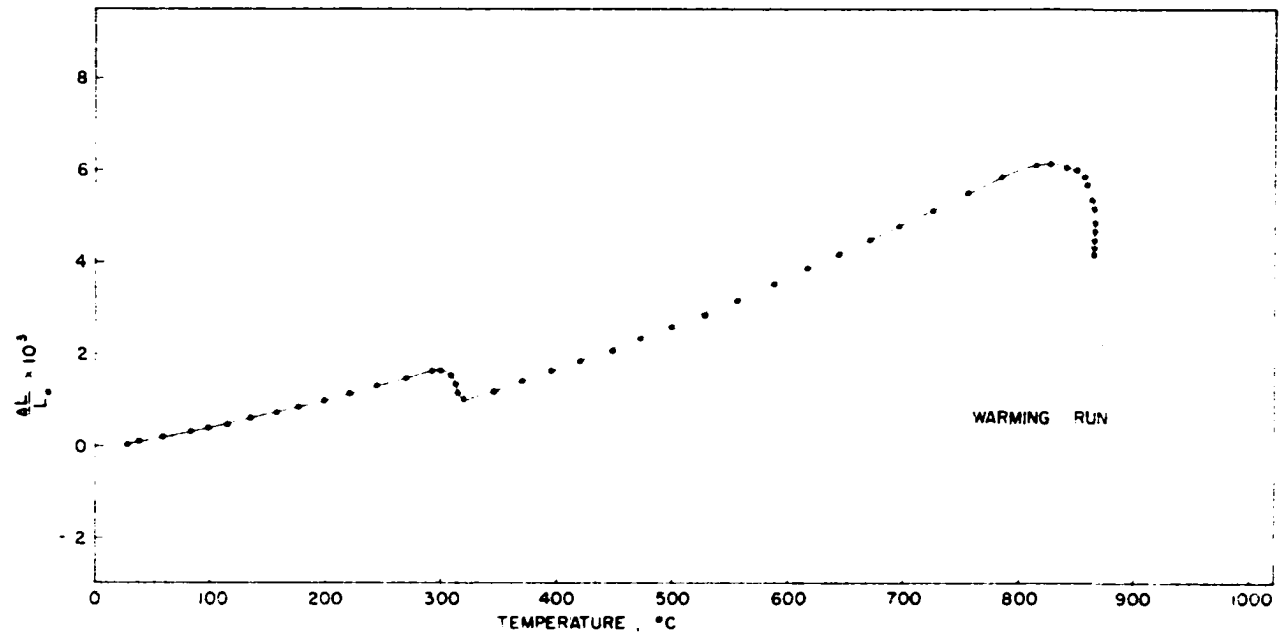

Figure 9. Thermal Expansion of Lanthanum, Run 2

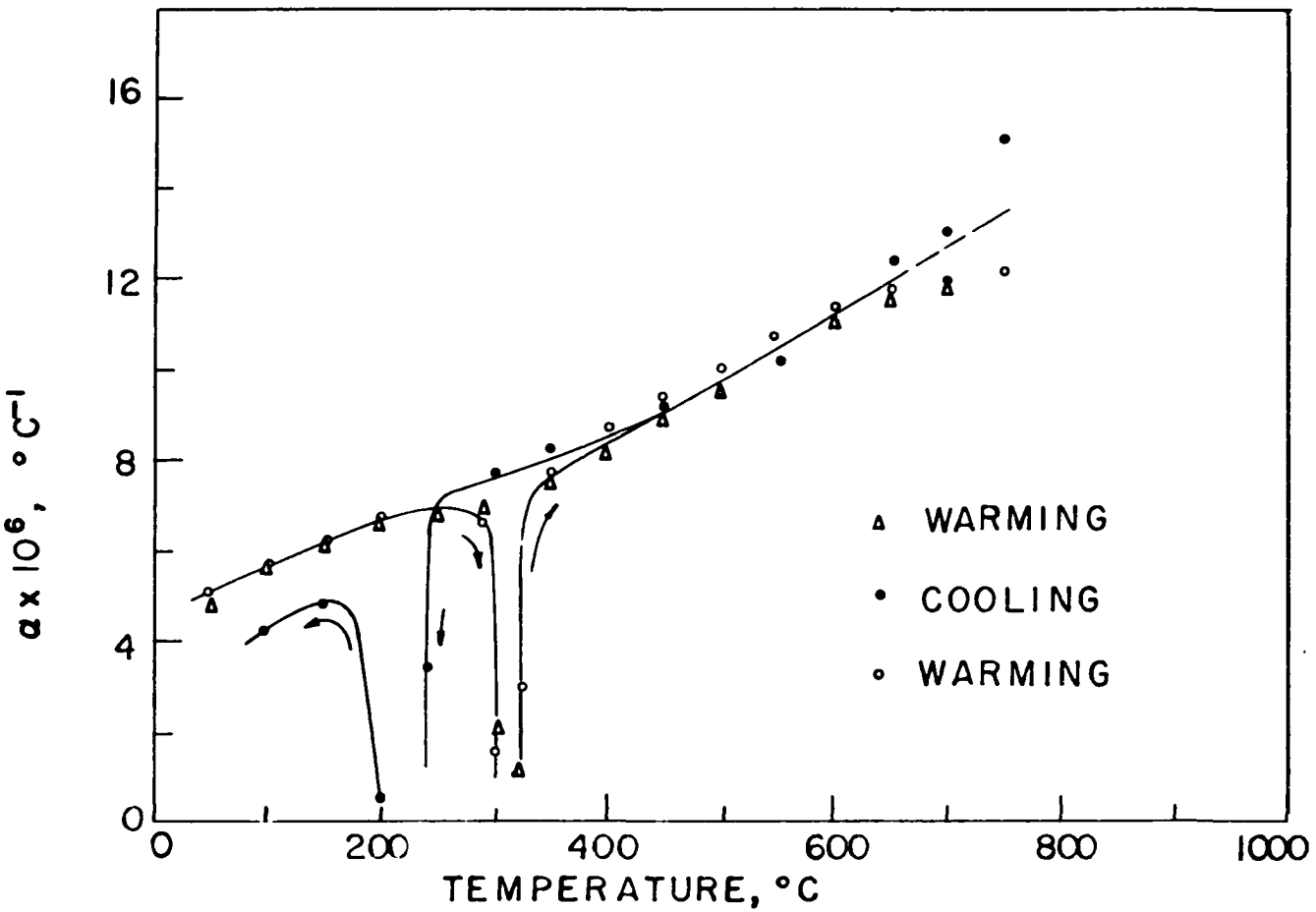

Figure 10. Expansion Coefficient of Lanthanum

Cerium

The coefficient of expansion of cerium is shown in Figure 11. Once more at the high temperature end there is considerable creep of the metal. Other determinations to higher temperatures showed an extreme flow similar to that in lanthanum, so that once more it was not possible to include the region of the high temperature anomaly reported in other studies.

Below about 200°C, cerium showed a negative curvature, that is, a decreasing slope, which is unusual for metals. This effect is better shown in Figure 12, where the expansion coefficient is seen to increase below 200°C. Reproducibility was good except in the regions near room temperature and at very high temperatures.

It is believed that the increase in the expansion coefficient near room temperature was due to the onset of the transition between the normal face-centered cubic and the condensed form. Although this transformation is largely a low temperature effect, there is evidence in other properties too that it probably "tails off" to high temperatures to some extent. The room temperature coefficient of expansion was about $8.5 \times 10^{-6}\ °C^{-1}$, although in the absence of the anomalous behaviour in this region, it might have been about $5.5 \times 10^{-6}\ °C^{-1}$, a value nearer to that of the neighboring rare earth metals.

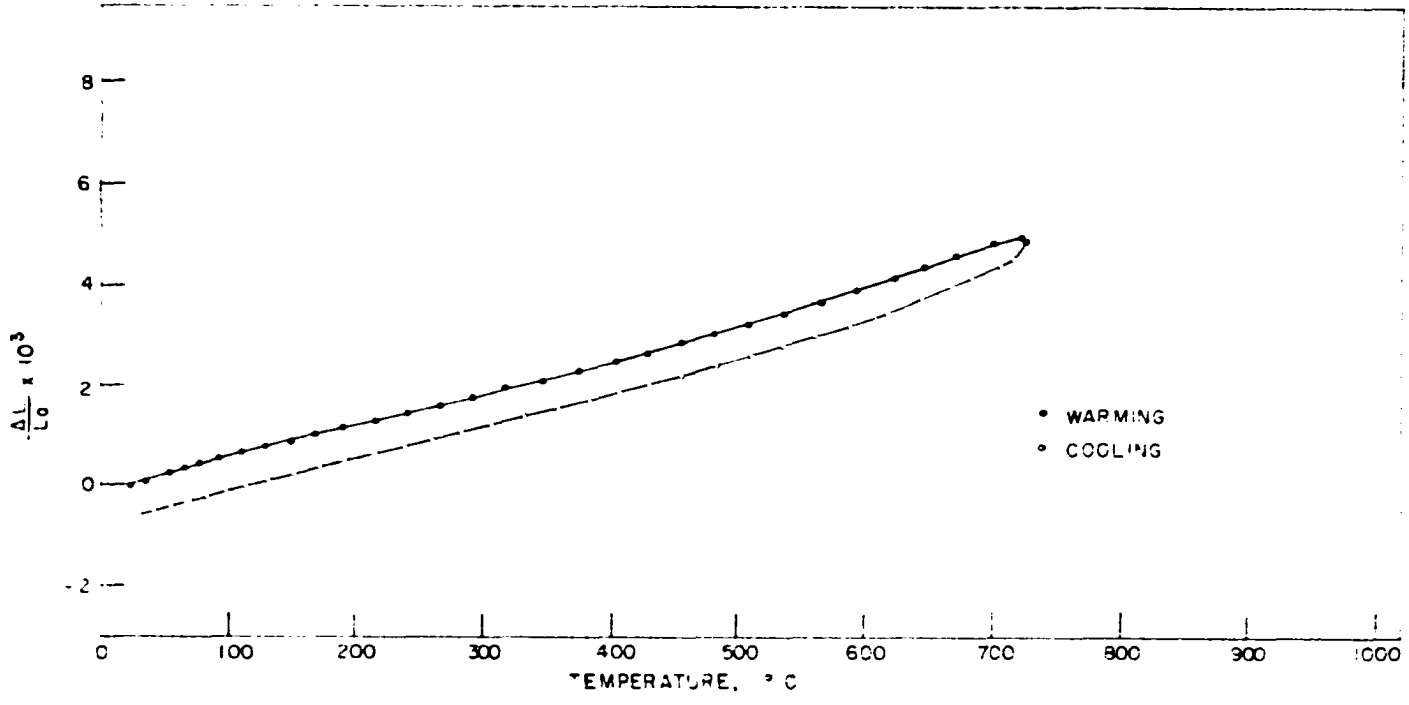

Figure 11. Thermal Expansion of Cerium

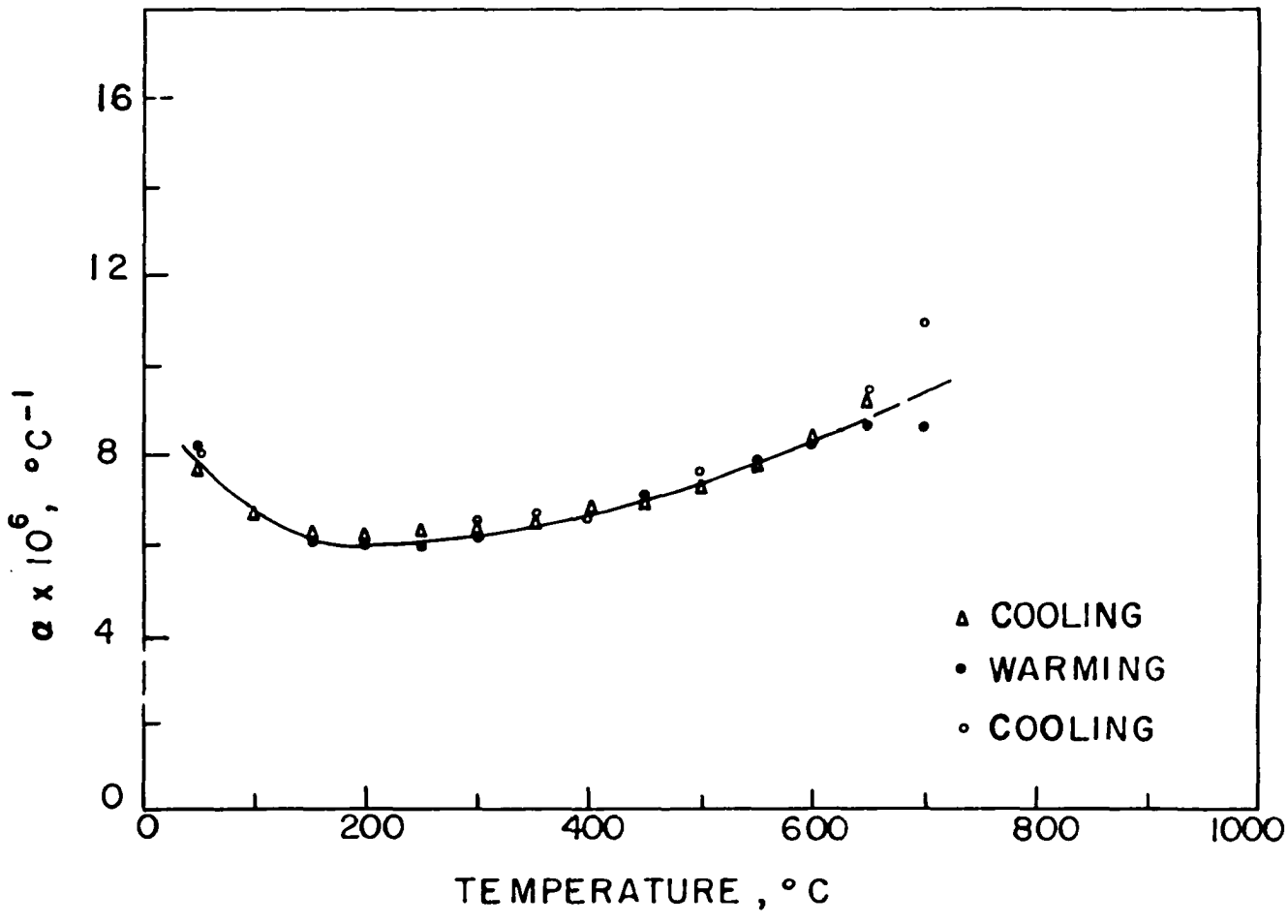

Figure 12. Expansion Coefficient of Cerium

Praseodymium

In the case of praseodymium it was finally possible to carry the experimental work through the range of the high temperature transition. Once again considerable creep occurred at the highest part of the run, but with the transition about 140°C below the melting point, this effect was not so great as to prevent the measurements from being made. The results are shown in Figure 13.

The high temperature anomaly is an extremely small one, so small, in fact, that the creep was sufficient to mask it almost completely in the warming direction. In the cooling runs, however, since the creep added to the thermal expansion rather than opposed it, the change in volume due to the transformation was readily observable. As found here, the anomaly occurred at 790° - 793°C, and involved a change in volume of only 0.1 per cent. This transition temperature agrees well with the 790° - 795°C reported by Herrmann (4) for the anomaly in electrical resistivity, and with the plateau in the cooling curve at 798°C as reported by Spedding and Daane (8). The effect is consistent with the general rule that transformations involving a volume increase are accompanied by an increase in electrical resistivity. It is rather surprising, however, that the dilatometric effect is so slight when the effects on resistivity and on the cooling curves are so great.

The coefficient of expansion of praseodymium is shown in Figure 14. The disagreement at high temperatures between

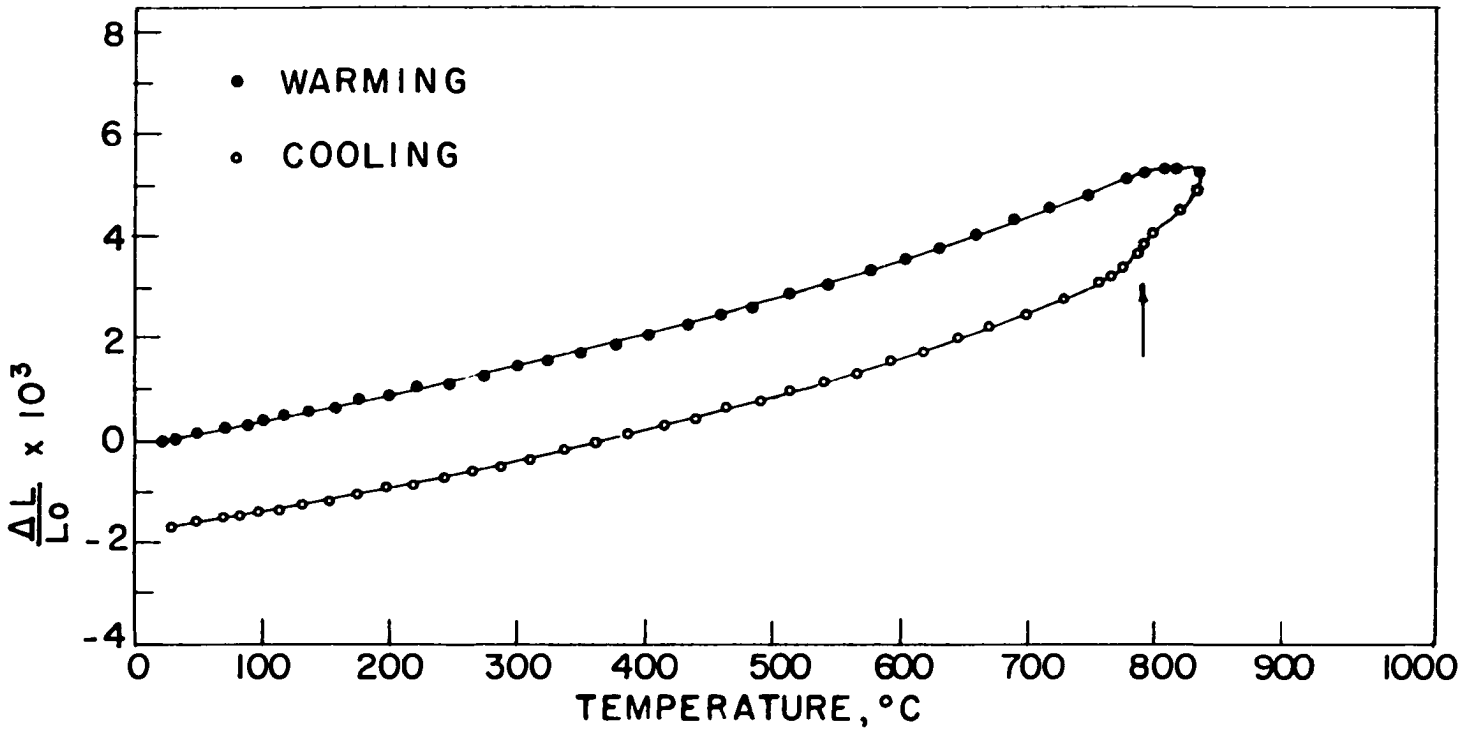

Figure 13. Thermal Expansion of Praseodymium

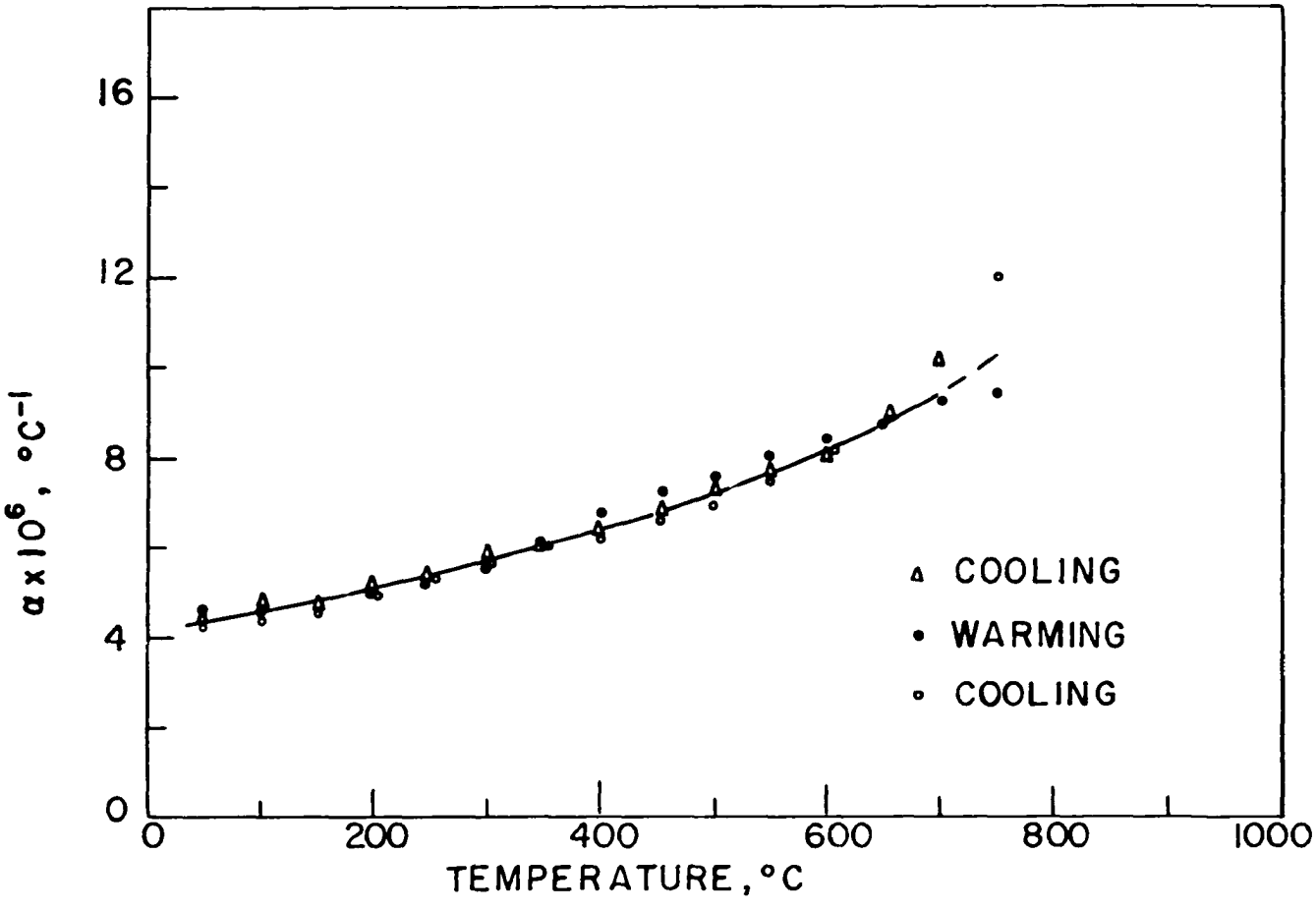

Figure 14. Expansion Coefficient of Praseodymium

the cooling and warming runs is simply the result of the creep which occurred in this region. The room temperature value, 4.2×10^{-6} °C^{-1}, is considerably less than the value previously found by Barson, Legvold, and Spedding (13), about 5.4×10^{-6} °C^{-1}.

Neodymium

Neodymium, whose high temperature transformation had been reported over 150°C below its melting point, offered another opportunity to make dilatometric measurements which would include this interesting region. The results of these measurements, shown in Figure 15, were similar to the results with praseodymium.

The temperature of the anomaly was about 867° ± 2°C, which agreed well with the thermal arrest found at 868°C by Spedding and Daane (8) and the anomaly of electrical resistivity at 861° - 863°C found by Herrmann (4). As with praseodymium, only a small volume change occurred, about 0.1 per cent.

There was no evidence of an anomaly in the region 600°C to 650°C as reported by Trombe and Foex (39) in their dilatometric study, unless this corresponded to the anomaly found so much higher in the present work. From a comparison of the nature of these anomalies, however, this seemed doubtful.

The expansion coefficient of neodymium is shown in Figure 16. The reproducibility was rather good even at

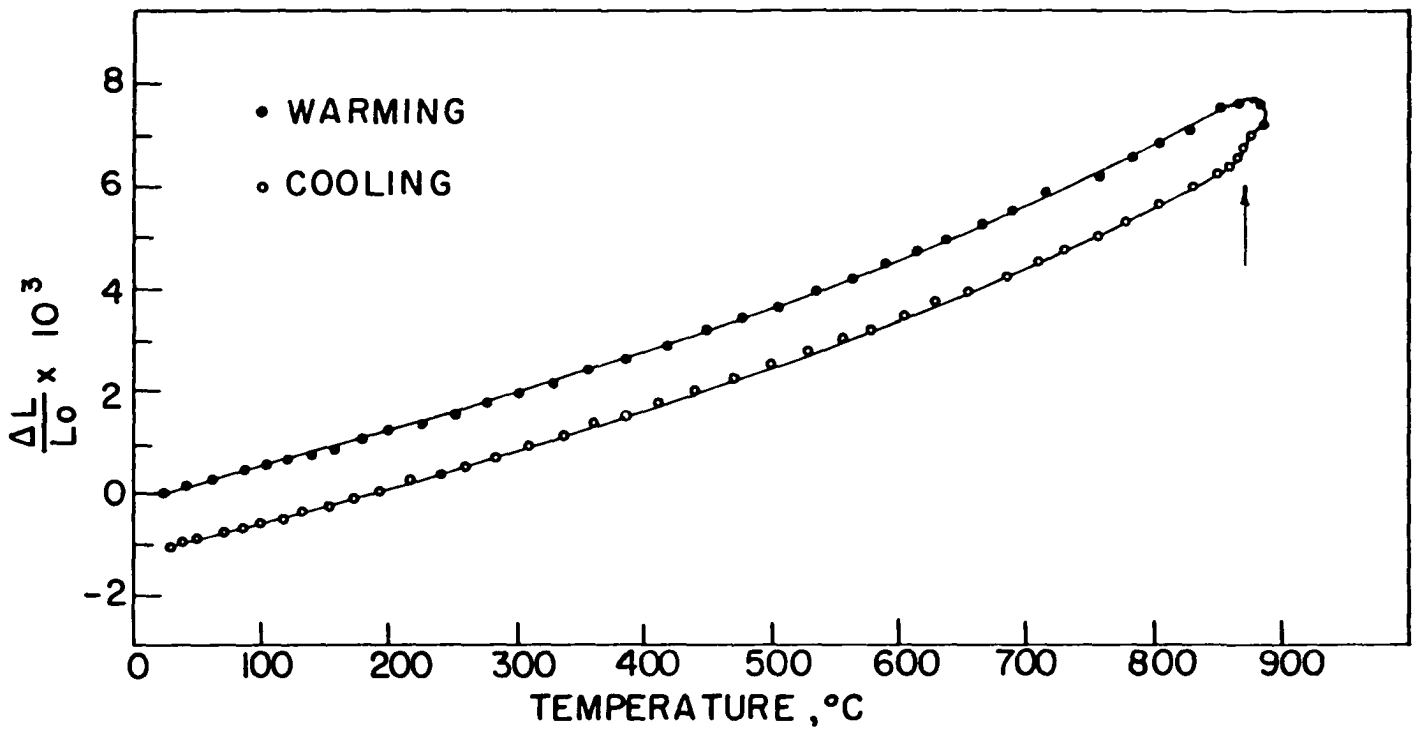

Figure 15. Thermal Expansion of Neodymium

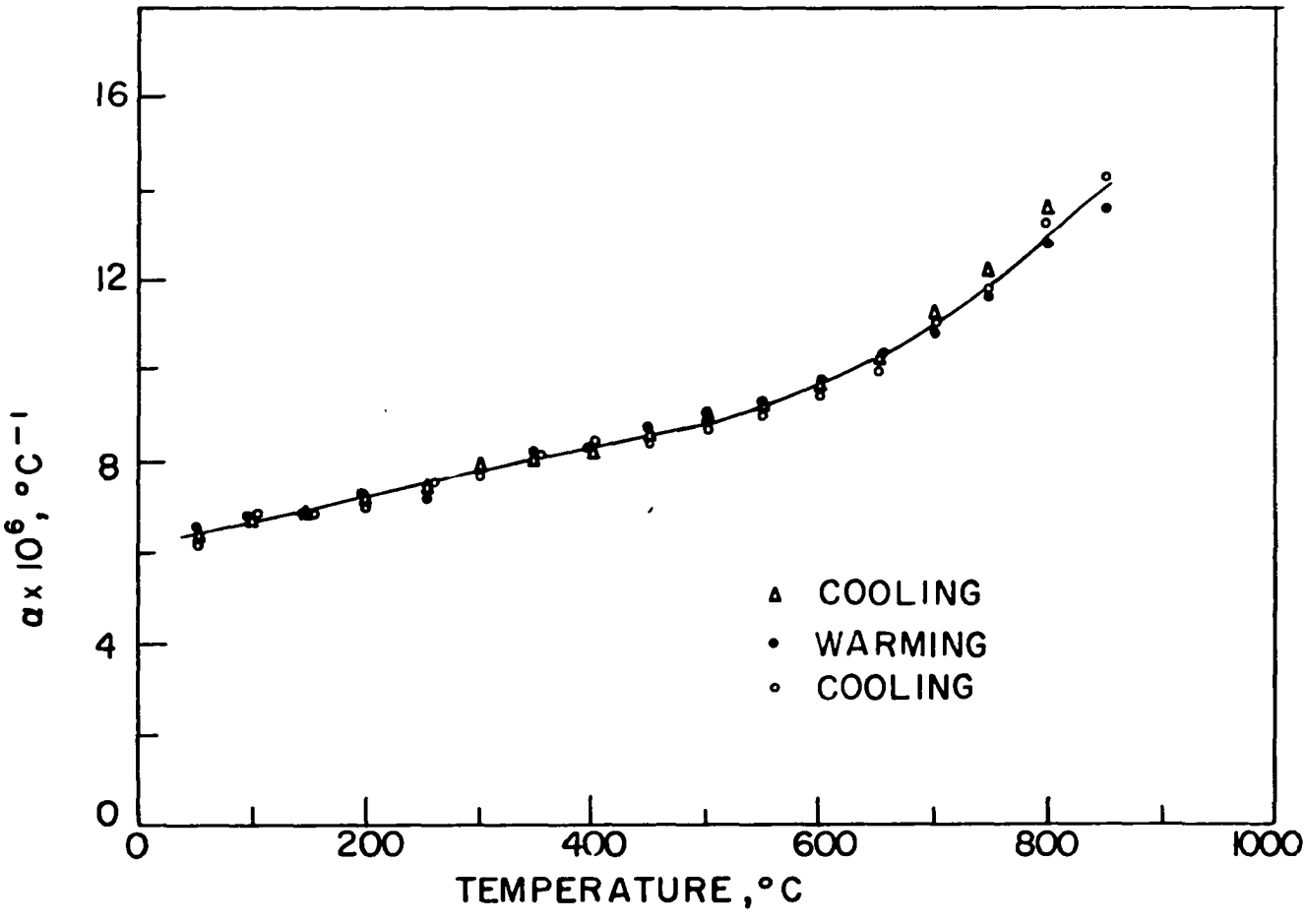

Figure 16. Expansion Coefficient of Neodymium

higher temperatures, since the amount of softening was not too great below about 850°C. A slight rise in the coefficient above about 650°C seemed to be fairly general for the higher melting rare earths in which this range could be covered. The room temperature coefficient of expansion was found to be about 6.3×10^{-6} °C^{-1}, which is in only fair agreement with Trombe and Foex's (39) value of about 7×10^{-6} °C^{-1} and Barson, Legvold, and Spedding's (13) value of 7.1×10^{-6} °C^{-1}.

Gadolinium

Since the Curie point of gadolinium is only slightly below room temperature, it was very desirable to try to include this range, as well as the high temperature region, in the investigation. With a plug in the bottom of the furnace, the power was left turned off and some liquid nitrogen poured into the furnace tube to cool it. The temperature was allowed to rise normally until the rate of warming became inconveniently slow, and then the furnace was turned on to increase the temperature more rapidly. The temperature control was poor by this method, the rate of warming being very rapid below -100°C especially. Since the equipment was not properly tested and calibrated in this range either, the results can only be claimed as semi-quantitative. It is believed that they are fairly accurate above -50°C, however, and qualitatively correct over the entire region covered.

The expansion of gadolinium, including this low temperature region, is shown in Figure 17. For a fairly large range, between -40°C and +28°C, the sample contracted with rising temperature; that is, the coefficient was negative. This is opposite to the behaviour of the classical ferromagnetics in which the expansion is enhanced by an additional positive quantity upon passing through the Curie point. The data of Trombe and Foex (46) exhibited a long plateau, or region of zero expansion, below the Curie point. This is still in fairly good agreement with the present work, considering the fairly small size of the effect.

The expansion coefficient, shown in Figure 18, seemed to indicate the beginnings of this effect, however slightly, at temperatures as high as 150°C or 200°C. In the high temperature region, the rather sharp increase of the coefficient above about 600°C was again evident. The reported slight transformation with hysteresis, found by Trombe and Foex (46) between 100°C and 200°C, was not confirmed by the present work.

Terbium

For terbium, with a Curie point tentatively identified at about -40°C, the method described above for achieving low temperature measurements was again of value. The same remarks regarding the accuracy in this range apply, however. The resulting expansion curve is shown in Figure 19. Again

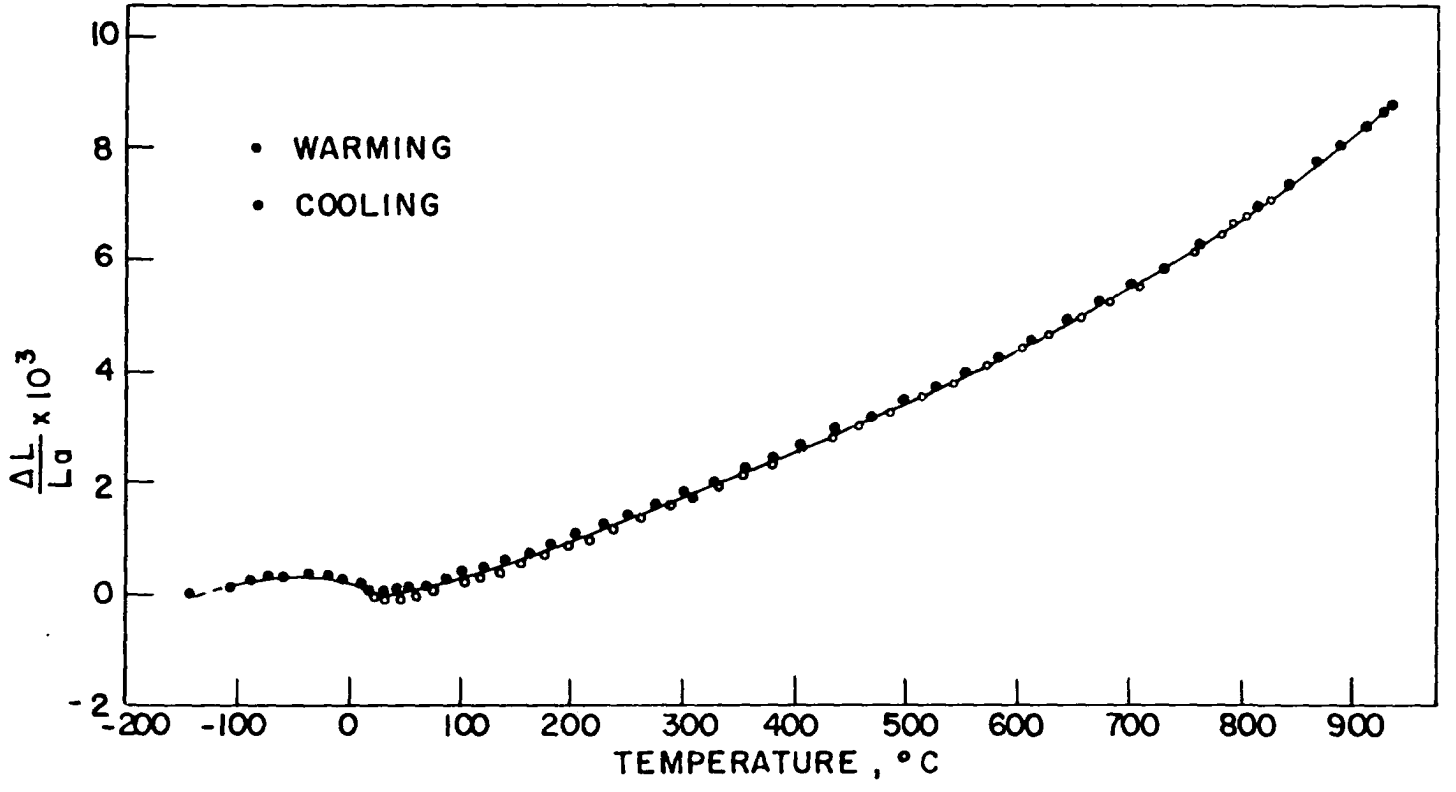

Figure 17. Thermal Expansion of Gadolinium

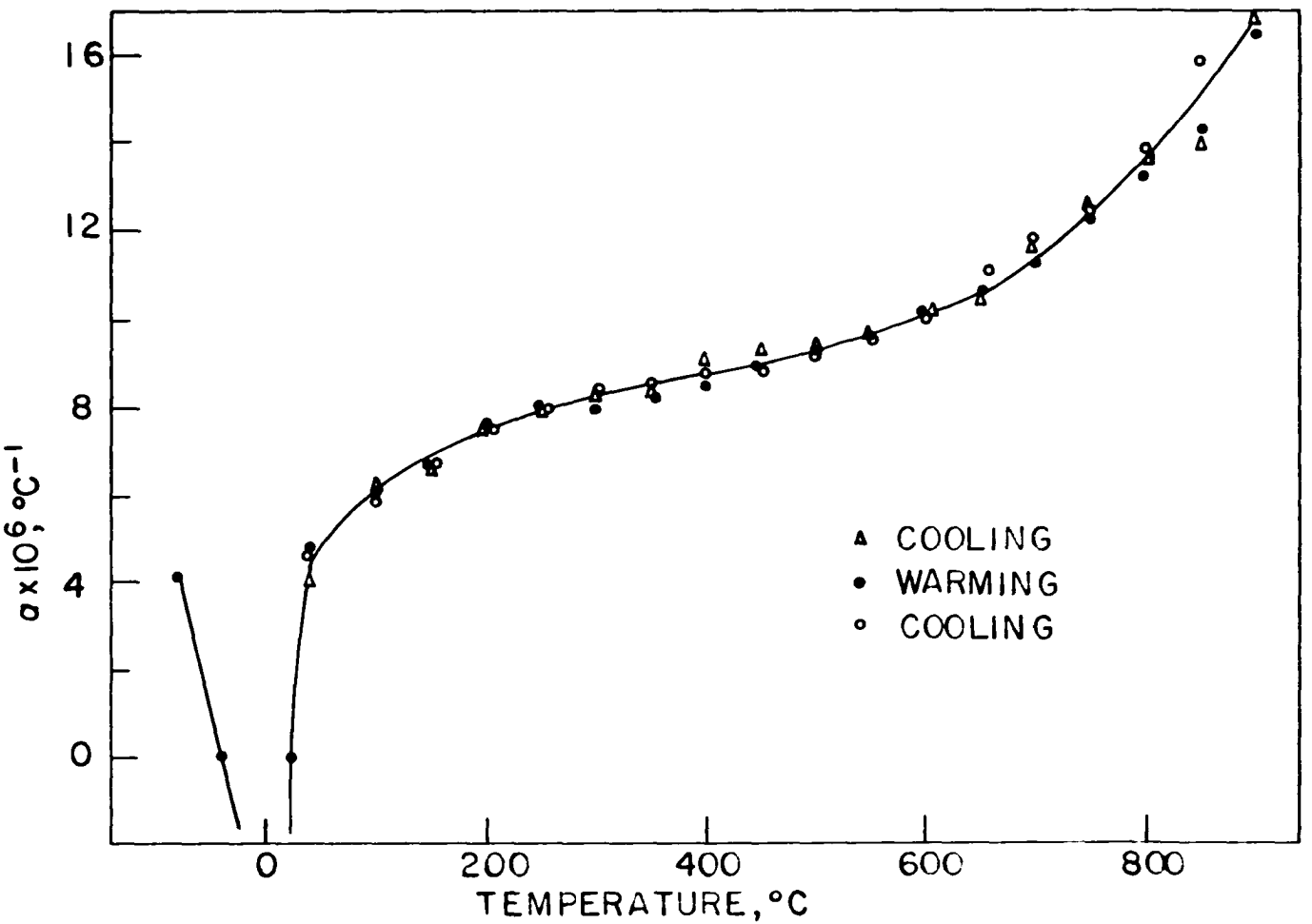

Figure 18. Expansion Coefficient of Gadolinium

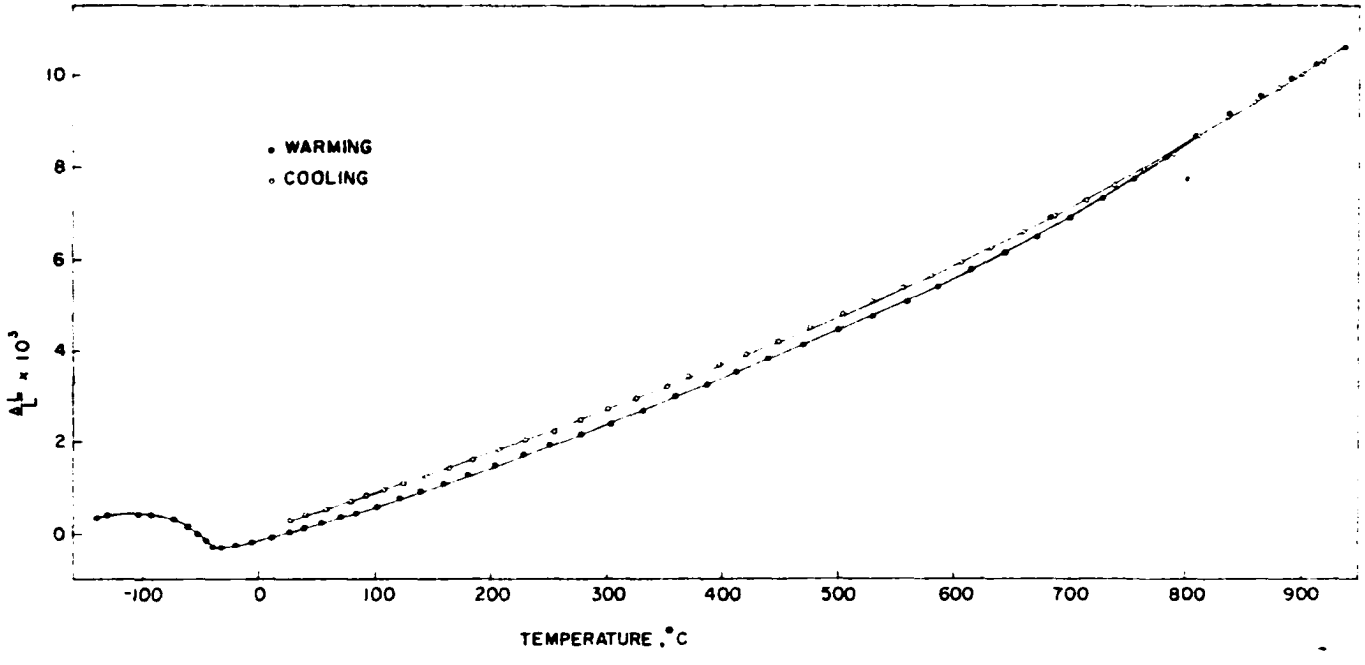

Figure 19. Thermal Expansion of Terbium

it is seen that a region of negative expansion appeared, the contraction being even more pronounced here with increasing temperature than in the case of gadolinium. By analogy with the expansion of gadolinium, one might expect that the Curie point is indeed in the neighborhood of -40°C, although of course the Curie point is actually defined magnetically rather than by anomalous behaviour in other physical properties.

In the high temperature region, a discrepancy appeared in the curves over the region from 700°C to 800°C. The data were not reproducible to the usual degree, and while the discrepancy seemed too slight to indicate a true transformation, still it seemed also too great to ignore. It seems most likely that stresses were introduced when the sample was rapidly cooled for the low temperature work, and that the anomaly observed is an annealing process.

The expansion coefficient of terbium is shown in Figure 20. The anomalous behaviour at high temperatures is grossly exaggerated by such a plot. Elsewhere the data are smooth and reproducible but indicate once more that the oncoming magnetic transformation seems to affect the expansion of the metal over a surprisingly large temperature interval.

Dysprosium

The expansion of dysprosium above room temperature is shown in Figure 21. A slight hysteresis loop was observed between about 650°C and 900°C. The change in volume

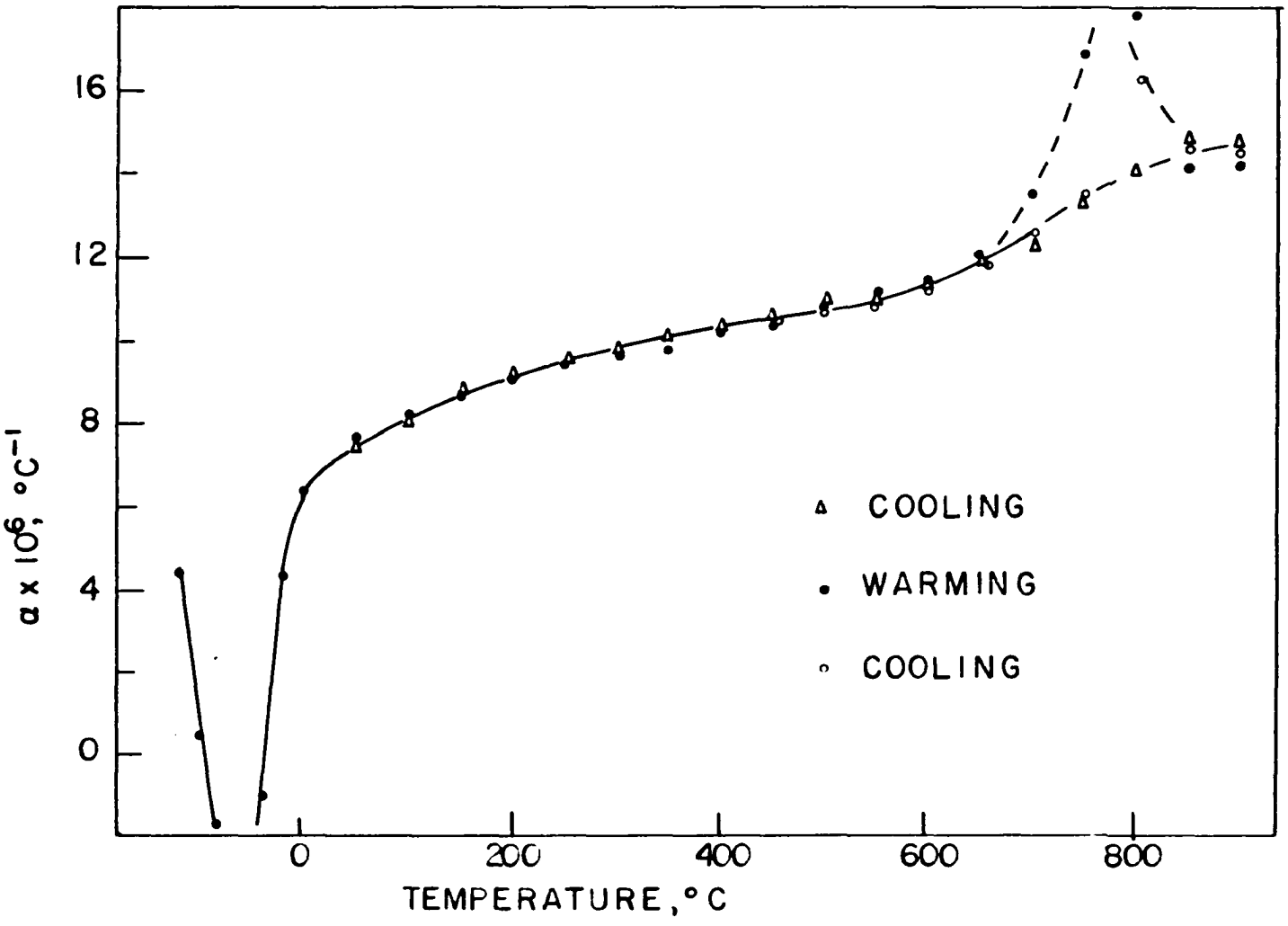

Figure 20. Expansion Coefficient of Terbium

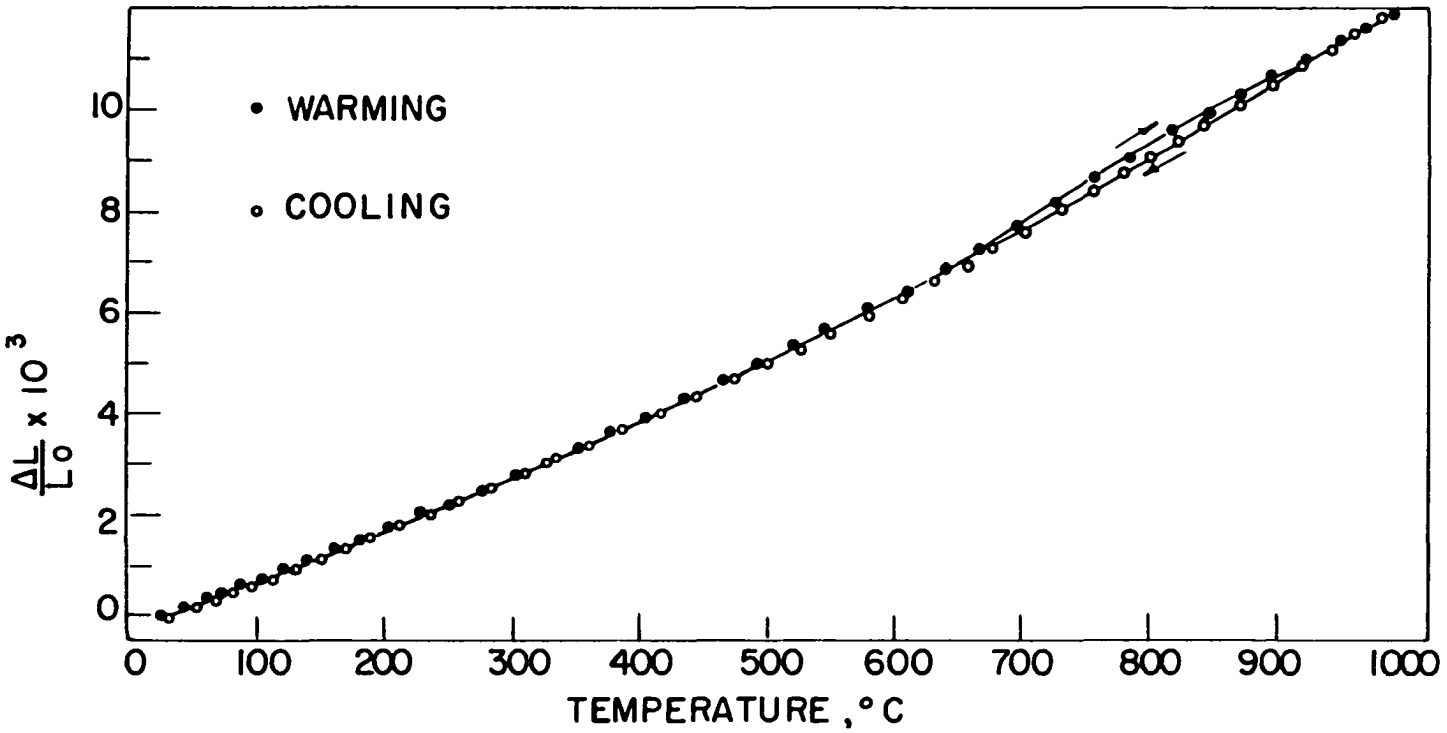

Figure 21. Thermal Expansion of Dysprosium

represented by this anomaly was not sharp and was more noticeable in the warming than in the cooling runs. A change in volume of less than 0.1 per cent was involved. Here again it would be of interest to see studies of other physical properties made, particularly a high temperature X-ray crystal analysis, if possible. Figure 22, the coefficient of expansion of this metal, shows that the runs were smooth and reproducible outside of the high temperature region mentioned. A room temperature coefficient of expansion of about 9.5 x 10^{-6} $°C^{-1}$ was indicated. This was considerably higher than the values reported by Trombe and Foex (50) and Barson, Legvold, and Spedding (13), who found the room temperature value around 8 x 10^{-6} $°C^{-1}$. It might be recalled that the spectroscopic analysis of the present sample of dysprosium indicated 0.5 per cent tantalum, 0.2 per cent calcium, and perhaps 0.1 per cent terbium. This relatively high impurity content may have affected the expansion of the sample.

Erbium

The expansion of erbium, shown in Figure 23, was gratifyingly smooth and reproducible. No evidence was observed of any transformations between room temperature and 900°C.

Figure 24 shows the expansion coefficient of erbium. Its room temperature value was found to be 9.4 x 10^{-6} $°C^{-1}$, which is in fairly good agreement with 8.9 x 10^{-6} $°C^{-1}$ observed by Barson, Legvold, and Spedding (13) and with the

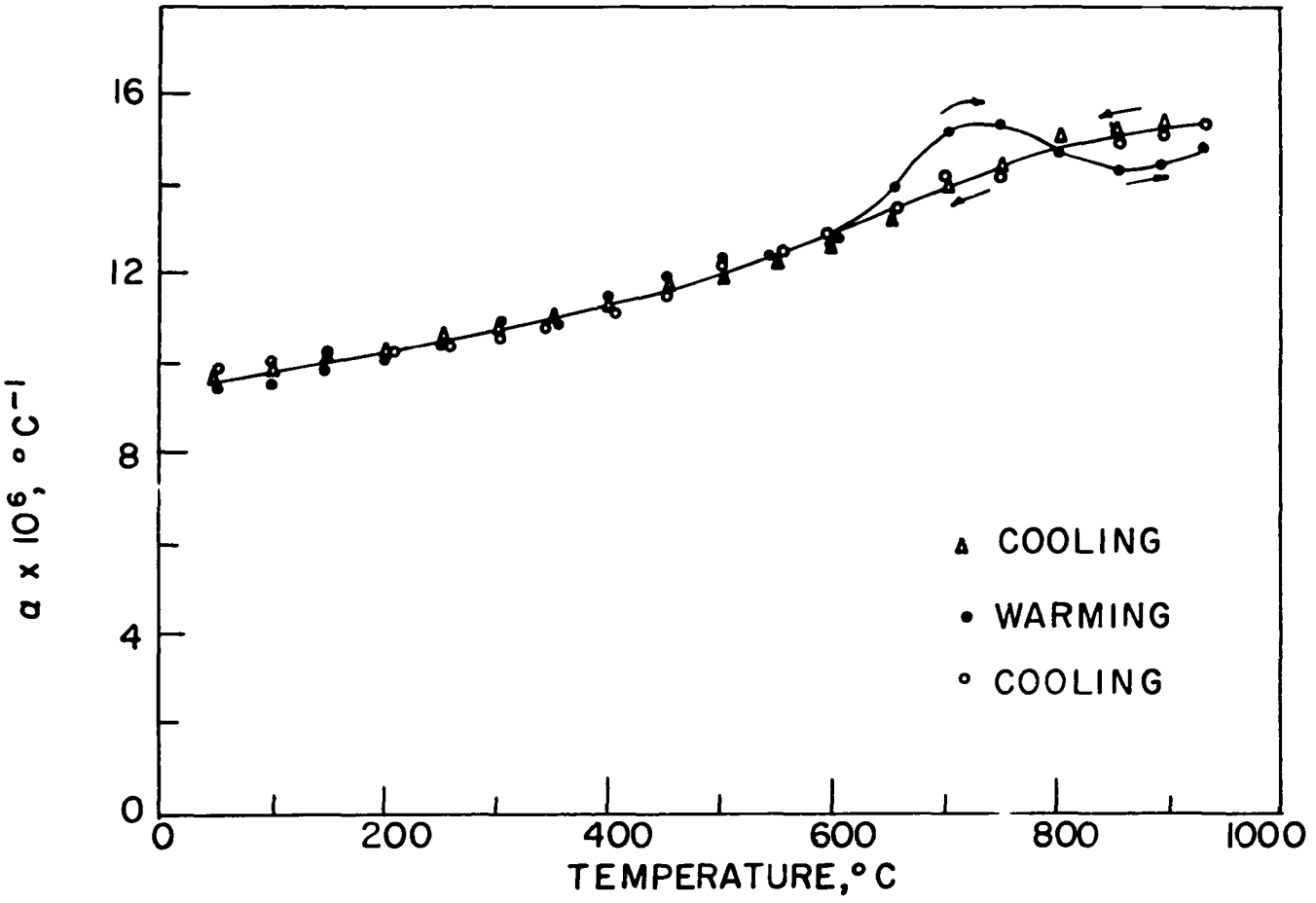

Figure 22. Expansion Coefficient of Dysprosium

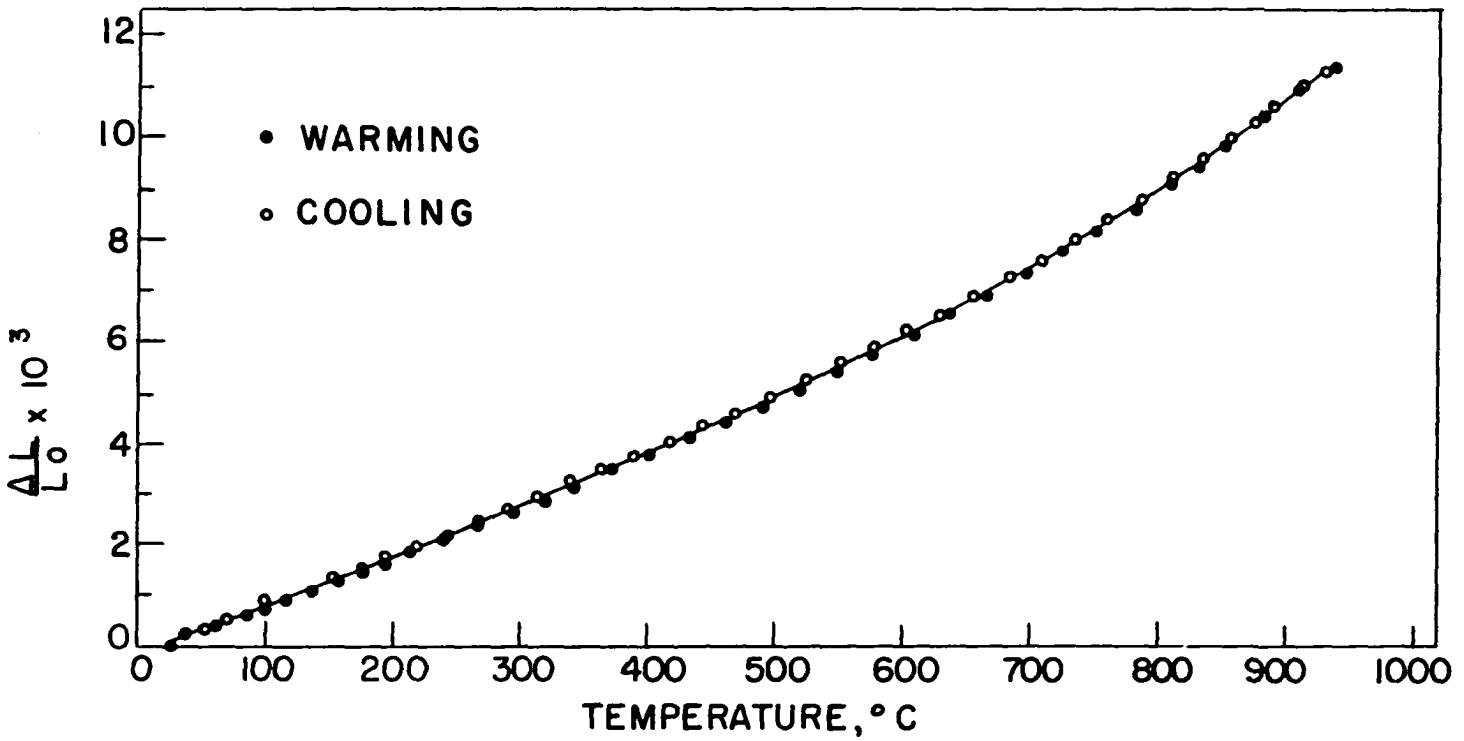

Figure 23. Thermal Expansion of Erbium

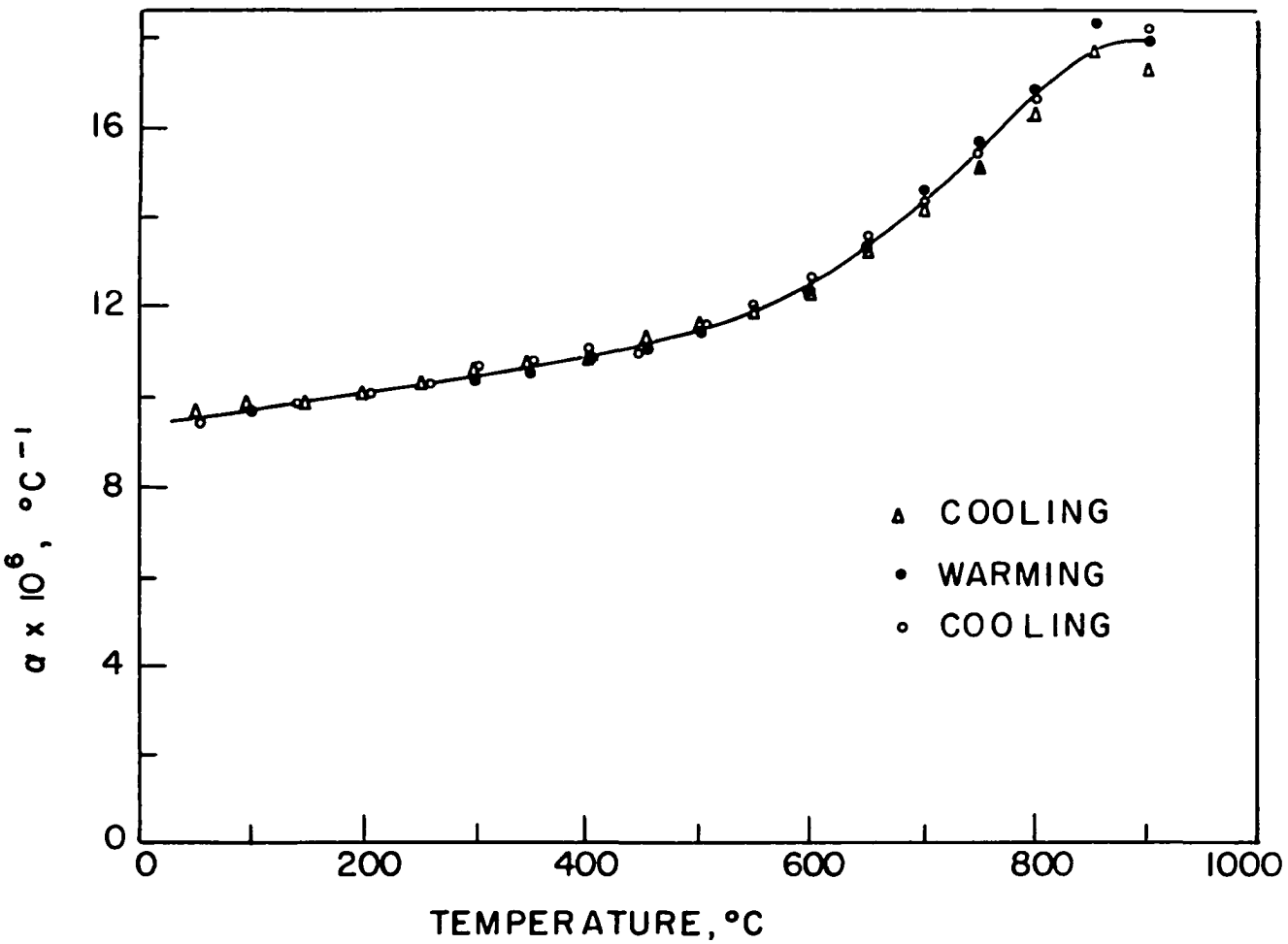

Figure 24. Expansion Coefficient of Erbium

estimate of 10 x 10^{-6} $°C^{-1}$ from the X-ray crystallographic data of Banister, Legvold, and Spedding (41).

Ytterbium

The least satisfying results of all were obtained with ytterbium. As seen in Figure 25, there was appreciable scattering of the points about a smooth curve, and also a very strange anomaly at high temperatures. The second cooling run was unfortunately interrupted by a failure in the electrical parts of the recording equipment so that only a small portion of this run was obtained. Over this portion, however, down to about 700°C, the results were identical with the first cooling run.

In performing this experimental work it was believed from the appearance of the strip chart at the high temperature end that the sample had softened and was showing signs of creeping. However, when the expansion curve was plotted and showed no net shortening of the sample upon its return to room temperature, this seemed to indicate that a true transformation was occurring at high temperatures. The highest temperature attained was still at least 25°C below the thermal arrest detected at 798°C by Spedding and Daane, although the anomaly observed may have corresponded to this transformation.

Ytterbium, with its very high vapor pressure, was extremely volatile during the high temperature part of the run,

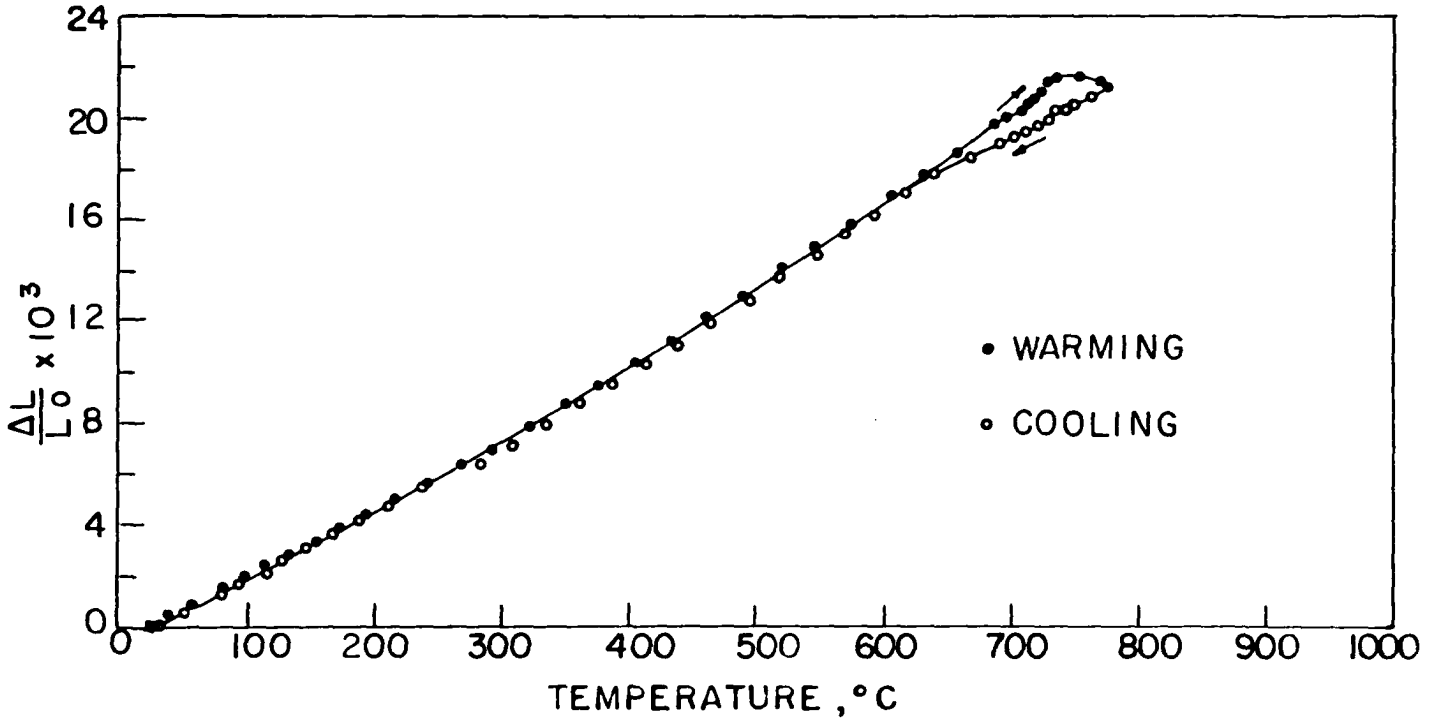

Figure 25. Thermal Expansion of Ytterbium

and a quantity of the metal was deposited as tiny crystallites in the cooler portions of the sample holder. There still remains the possibility that this interfered with the proper operation of the dilatometer. It would seem desirable to repeat these measurements to check the observed data, but in view of the high volatility of the sample, it was thought best first to complete the use of the equipment on other samples.

The expansion coefficient, shown in Figure 26, was extremely high for a rare earth metal. The room temperature value of $25 \times 10^{-6}\ ^{\circ}C^{-1}$ is about three times that of other elements in this group. In view of the differences in other physical properties which this element exhibits, and its chemical divalence compared to the usual trivalence of most rare earths, this is perhaps not too unexpected.

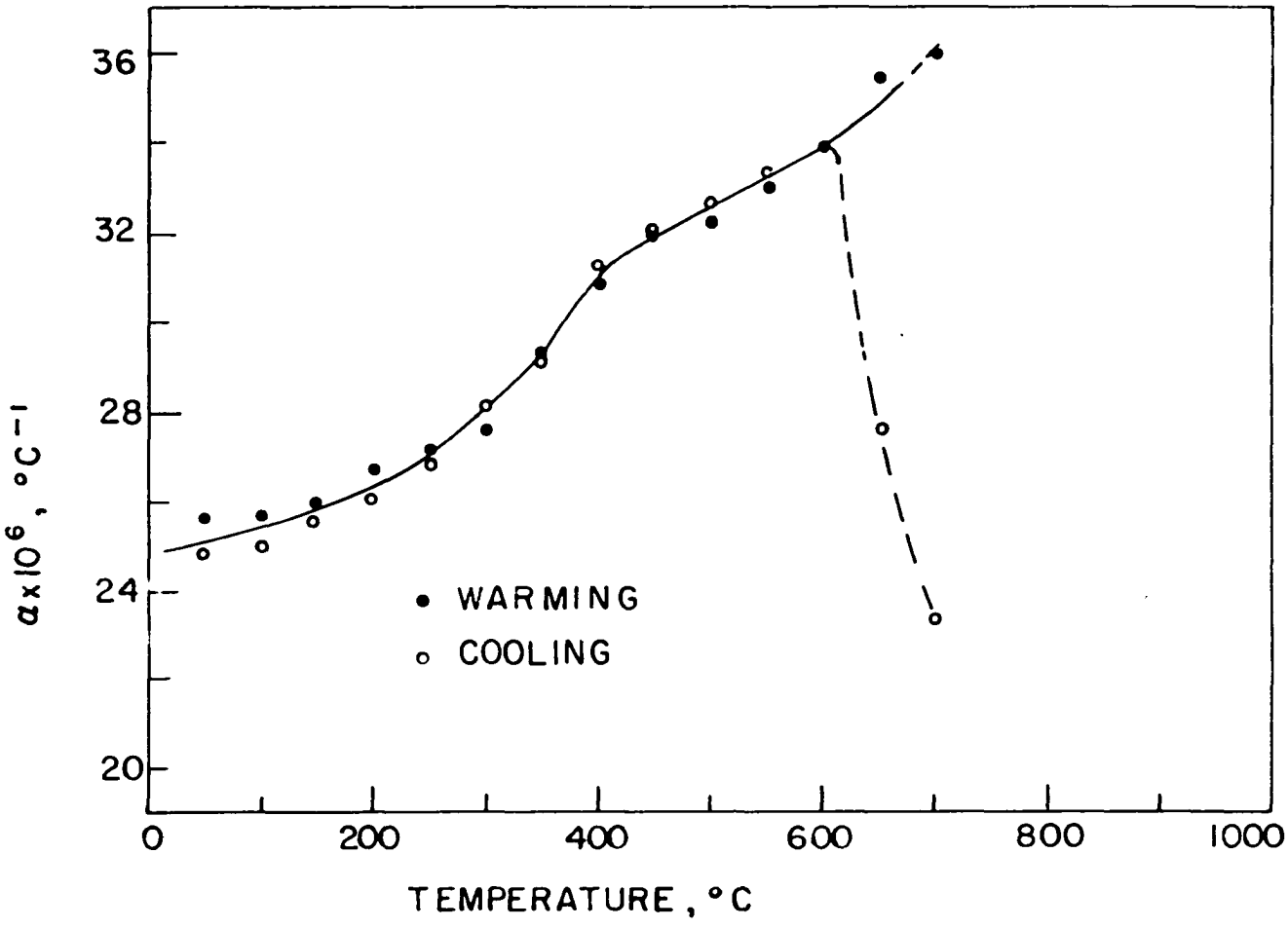

Figure 26. Expansion Coefficient of Ytterbium

DISCUSSION

High Temperature Creep

The phenomenon of creep has been a subject of lively interest among physicists and metallurgists for some time. In view of the flow of several of the rare earths at high temperatures, a few comments on creep in metals are appropriate.

Andrade (75) found that the change in length of a metal as a result of creep under tension followed the expression $L = L_o(1 + \beta t^{1/3})\, e^{kt}$, where L_o and L are the lengths at time zero and time t respectively and β and k are constants at a given temperature and stress. The term $\beta t^{1/3}$ represents a rapidly decreasing flow called transient flow or β flow. The term in k arises from a constant rate of flow per unit length $\frac{1}{L}\frac{dL}{dt} = k$. Since k is usually quite small, this is approximately a uniform increase of length with time and is called quasi-viscous flow. As the stress or temperature is increased, the value of β increases somewhat but then levels off to a fairly constant value. The value of k, however, increases rapidly and continuously as the temperature or stress is increased. Hence, at elevated temperatures it is the viscous flow which predominates. It is this which apparently is the cause of the permanent deformation observed in the present measurements on the rare earth metals.

A review of earlier papers on the mechanism of creep was given by Nabarro (76). The process of transient creep was

found to occur largely by slip in the individual grains and is usually explained as due to the motion and interaction of dislocations within the crystal. Quasi-viscous creep involves a motion of the individual grains relative to each other and hence involves the grain boundary.

As Orowan (77) pointed out, however, quasi-viscous creep also occurs in single crystals, so that a mechanism involving the structure of the grains themselves must also be involved. More recently Betteridge and Franklin (78), by deforming a sample of a tin-antimony alloy and examining it microscopically, found three distinct phenomena: viscous flow at the grain boundaries, general slip within the grain, and localized strain within the grain which resulted in a subdivision of the grains into a "cell structure".

These phenomena, involving dislocations, lattice vacancies, and other crystalline imperfections, might well explain the extremely diffuse X-ray diffraction patterns obtained from the rare earth metals. The surprising thing here was that the creep rate should be so great for as small a load as the sample was subjected to in the dilatometer. It may be that the high temperature transition, with its accompanying recrystallization, resulted in an increase of disordered material in the metal. This would be consistent with the large changes in the electrical resistivity and in the cooling curves found for these metals.

Expansion and the Curie Point

A review of material dealing with expansion in the neighborhood of the ferromagnetic Curie point is given by Bozorth (79). The following remarks, except where otherwise noted, are taken from this source, which also includes a list of references.

The subject is conveniently discussed in terms of Bethe's curve showing the exchange integral of magnetization as a function of $\frac{R}{r}$, where R is the atomic radius and r is the radius of the incomplete inner electronic shell associated with the ferromagnetism. At small values of this ratio (atoms close together compared to the radius of the unfilled shell) Bethe's calculations showed the exchange integral to be negative, corresponding to a tendency towards anti-parallel alignment of the electron spins in adjacent atoms, or antiferromagnetism. For values of $\frac{R}{r}$ greater than about 1.5, however, the exchange interaction becomes positive, corresponding to parallel spin alignment, or ferromagnetism. The interaction reaches a positive maximum for some value of $\frac{R}{r}$ greater than 1.5 and then decreases to zero asymptotically as the distance between atoms becomes large compared to the radius of the incomplete inner shell of electrons.

Ferromagnetic materials must have a positive exchange interaction, but they may lie either to the right or to the left of the maximum in Bethe's interaction curve. For metals lying to the left of the maximum, a decrease of the atomic

radius, such as by compression, would cause a decrease in the magnitude of the exchange integral and hence a lowering of the Curie point. For metals to the right of the maximum, pressure would cause an increase in the Curie point. Both cases have been observed experimentally.

One of Ehrenfest's equations for second order transition shows that at the Curie point $\alpha^F - \alpha^P = \frac{C_p^F - C_p^P}{3TV} \frac{dT}{dp}$. Here the superscripts refer to the ferromagnetic and paramagnetic states. Since $C_p^F - C_p^P$ is positive, it can be seen that the coefficient of expansion should be greater in the paramagnetic state for metals lying to the left of the maximum in Bethe's curve, and greater in the ferromagnetic state for metals to the right of the maximum. This follows from the pressure-dependence of the Curie point, as discussed in the preceding paragraph.

For gadolinium, the ratio of the atomic radius to the radius of the 4f shell is given by Bozorth as 3.1. This would place the metal rather far out to the right of the maximum on the interaction curve, and would predict a slight decrease in the expansion coefficient on passing through the Curie point in a warming direction. The experimental evidence found in the present investigation, as well as that of Trombe and Foex (46) showed the effect to be just opposite to this. From the arguments above, this indicates that gadolinium should really lie to the left of the maximum in the interaction curve. Terbium, with its negative coefficient of

expansion in the region of the Curie point, should also be located to the left of the maximum in the curve.

Zener and Heikes (80) have enumerated several types of exchange other than direct exchange between the incomplete shells. It seems that in the case of the rare earths, where the incomplete shell is buried rather deeply in the atom, that indirect exchange would occur and that one may no longer locate the metal correctly on the interaction curve relative to metals of the iron group by calculating $\frac{R}{r}$ for the 4f shell. Perhaps using the radius of the incomplete 5d shell would reduce the value of $\frac{R}{r}$ to place gadolinium and terbium to the left of the maximum.

Another effect which was noted with regard to the results of the present investigation was that the expansion coefficient was evidently affected by the loss of magnetism over a range extended more than a hundred degrees above the true Curie point. It is interesting to note that a similar effect was observed by Nix and MacNair (65) in the expansion of iron and nickel and by Mott and Potter (81) in the temperature coefficient of electrical resistivity of nickel. The last authors explained this as being due to something like short range order which remains after the breaking up of the large Weiss domains at the Curie point, the last bit of this order vanishing gradually at higher temperatures. A similar "tailing off" of the magnetism itself above the Curie point is described by the Curie-Weiss law.

The Grüneisen Constant

All of the physical constants for determining the Grüneisen constant, $\gamma = \frac{3\alpha V}{C_v k}$, have been experimentally measured for several members of the rare earth group. Bridgman (57) measured compressibilities and densities, and the present investigation, as well as others previously, supplied thermal expansion data. Atomic heats were obtained from the results of Parkinson, Simon, and Spedding (24) by a rather bold extrapolation to room temperature, and from the data of Skochdopole, Griffel, and Spedding (55, 45). Room temperature values of these physical properties were used except in the cases of gadolinium and cerium where higher temperature values were used to avoid the effect of transitions. It was assumed that the compressibilities changed but little with temperature. The resulting Grüneisen constants for several of the metals are listed in the column headed γ_{Gr} in Table 1.

It is seen that the values ranged from 0.25 for cerium to 0.90 for erbium, all of which are very much less than the usual value of about 2.0 for most metals. In view of this discrepancy, a second method for calculating the Grüneisen constant, due to Slater (82), was employed. If the compressibility of a substance is expressed as a function of pressure in the form $\frac{\Delta V}{V_o} = -a_1 P + a_2 P^2$, where V is the volume, P the pressure, and a_1 and a_2 are constants, then it can be shown that $\gamma = \frac{a_2}{a_1^2} - \frac{2}{3}$. With a few exceptions, the values

Table 1. Grüneisen Constants of Several Rare Earth Metals

Metal	γ_{Gr}	γ_{Sl}
La	0.29	1.6
Ce	0.25	-11.
Pr	0.27	0.8
Nd	0.42	1.0
Gd	0.63	1.5
Dy	0.74	1.2
Er	0.90	1.2

of γ determined in these two independent ways are generally in fairly good agreement and range from about 1.5 to 2.5.

The coefficients a_1 and a_2 were determined approximately from Bridgman's compressibility data (57) and the resulting Grüneisen constants, γ_{S1}, are listed in the last column of Table 1. In the case of cerium, the large negative value indicates that the compressibility increased rapidly with increasing pressure rather than decreasing normally. This was doubtless due to the oncoming transition to the condensed form, so that this value of γ_{S1} is not particularly meaningful. In the remaining cases the values are still somewhat below the values commonly found for metals, but are in much better agreement than those calculated from the other physical properties.

It is inconceivable that the experimental values could be in error by so large an amount. Assumptions made in the derivation of these expressions for Grüneisen's constant are that the modes of vibration of the lattice all vary as the inverse γ power of the volume, and that the Poisson ratio be independent of volume changes. It may be that one or both of these assumptions is poor for the rare earth metals.

Expansion and the Melting Point

Attempts to correlate the observed expansion of the rare earth metals with their melting points, as has been done for other metals, met with no more success than did the calculations of the Grüneisen constants.

Bonfiglioli and Montalenti (2) reported the empirical relationship αT_m = constant, where α is the room temperature coefficient of linear expansion and T_m is the melting point on the absolute temperature scale. For face-centered cubic metals they found that $\alpha T_m = 2.08 \pm 0.22$ per cent, while for hexagonal metals it was 2.05 ± 0.10 per cent. Of the face-centered cubic metals investigated here, the value for this product was found to be 0.60 per cent for cerium, ignoring the anomalous increase in the expansion coefficient at room temperature, and 2.7 per cent for ytterbium. For the hexagonal metals, the product αT_m was as follows: lanthanum, 0.57 per cent; praseodymium, 0.51 per cent; neodymium, 0.82 per cent; gadolinium, about 1.2 per cent, taking α above the anomalous room temperature value; terbium, about 1.5 per cent; dysprosium, 1.7 per cent; and erbium, 1.7 per cent. Except for ytterbium, the observed expansion is lower than that predicted from their melting points, particularly for the first members of the rare earth series. This may be due to the high temperature transitions, for the melting would then occur from a different crystalline form. However, since the relationship is only empirical in the first place, it may simply not be a general one.

SUMMARY

A high temperature dilatometric investigation of the rare earth metals was undertaken as part of a broad program of study of these elements, the ultimate goal being better understanding of metals in general. The more immediate goal, in addition to determining the coefficients of expansion quantitatively, was to detect evidence of any crystalline transformations which may occur and particularly to cast some light on certain high temperature transitions already discovered in several of these metals. The rare earth metals included in this investigation were lanthanum, cerium, praseodymium, neodymium, gadolinium, terbium, dysprosium, erbium, and ytterbium.

In view of the highly reactive nature of these elements at high temperatures and their relatively small thermal expansion, it was necessary to design and build a somewhat specialized dilatometer. The device employed consisted essentially of a quartz-tube and dial-indicator dilatometer in which an optical interferometer replaced the dial-indicator gauge. This increased the sensitivity of the instrument and made possible automatic recording of the results by means of a photomultiplier tube which detected motion of the interference fringes. Provision was also made for controlling and recording the sample temperature automatically and for placing an inert atmosphere about the sample during the course of the run. It was estimated that this apparatus was capable

of determining the coefficient of expansion to about $\pm$ 0.2 x 10^{-6} $°C^{-1}$, some 2 or 3 per cent of the value for a typical rare earth metal.

Room temperature values of the coefficients of expansion, except in the case of ytterbium, were found to range from 4.2 x 10^{-6} $°C^{-1}$ for praseodymium to 9.5 x 10^{-6} $°C^{-1}$ for dysprosium. For ytterbium, a metal which assumes a divalent chemical form in compounds and generally has properties differing from most other members of the rare earth series, a room temperature coefficient of 25 x 10^{-6} $°C^{-1}$ was observed.

An indication of the hexagonal to face-centered cubic transformation in lanthanum appeared as a volume change, with hysteresis, between about 200°C and 320°C. The higher temperature face-centered cubic modification was formed with an accompanying decrease in volume of some 0.3 per cent.

It was found that in the lower melting metals an excessive amount of creep developed at high temperatures, due, it was thought, to a rapid increase in the number of lattice imperfections. This creep was so great that it was impossible to take usable data through the regions of the high temperature transitions of lanthanum and cerium. In the cases of praseodymium and neodymium, however, evidence of high temperature transitions could be observed. These appeared as very slight volume changes, the higher temperature form of both metals being about 0.1 per cent larger by volume than the modification below the transformation temperature. In

praseodymium this anomaly occurred at 790° - 793°C, while in neodymium it took place at about 867°C.

Since the Curie points of gadolinium and terbium had been reported not far below room temperature, an attempt was made to include this region in the study of these two metals by cooling the furnace prior to the runs. It was found that both of these metals exhibited a negative coefficient of expansion over a range of temperatures near to their reported Curie points, gadolinium from -40°C to +28°C, and terbium from -100°C to -40°C.

Dysprosium displayed a slight hysteresis loop in its expansion between 650°C and 900°C. Ytterbium apparently underwent a transformation of some sort in the high temperature region; however, the very high volatility of this metal may have interfered with the operation of the instrument, and this conclusion must be labeled as somewhat tentative for the present.

Attempts to calculate the Grüneisen constant from measured physical properties, including the expansion coefficients, resulted in values which were extremely low as compared with other metals. A second calculation of the same constant from compressibility data gave results which were somewhat higher, but still lower than the anticipated values. Attempts to correlate the thermal expansion of the rare earth metals with their melting points met with similar failure, the expansion being in most cases much lower than would be expected from comparison with other metals.

LITERATURE CITED

1. Grüneisen, E., in Henning, F., ed., "Handbuch der Physik" (Springer, Berlin, 1926), Vol. 10, p. 1.
2. Bonfiglioli, G. and Montalenti, G., J. Appl. Phys. 22, 1089 (1951).
3. Hidnert, P. and Souder, W., N.B.S. Circular 486 (U. S. Government Printing Office, Washington, D. C., 1950).
4. Herrmann, K. W. "Some Physical Metallurgical Properties of Scandium, Yttrium, and the Rare Earth Metals," Unpublished Ph.D. Thesis. Ames, Iowa. Iowa State College. (1955).
5. Vogel, R. and Heumann, T., Z. Metallkunde 38, 1 (1947).
6. Massenhaussen, W., Z. Metallkunde 43, 53 (1952).
7. Vogel, R. and Klose, H., Z. Metallkunde 45, 633 (1954).
8. Spedding, F. H. and Daane, A. H., J. Metals 6, 504 (1954).
9. Mendelssohn, K. and Daunt, J. G., Nature 139, 473 (1937).
10. Shoenberg, D., Proc. Cambridge Phil. Soc. 23, 577 (1937).
11. Jaeger, F. M., Bottema, J. A., and Rosenbohm, E., Rec. Trav. Chim. Pays-Bas 57, 1137 (1938).
12. Trombe, F. and Foex, M., Compt. Rend. 217, 501 (1943).
13. Barson, F., Legvold, S., and Spedding, F. H., Unpublished Research. Iowa State College. Ames, Iowa (1953).
14. Bridgman, P. W., Proc. Am. Acad. Arts Sci. 76, 65 (1948).
15. Bridgman, P. W., Proc. Am. Acad. Arts Sci. 81, 165 (1952).
16. Lawson, A. W. and Tang, T., Phys. Rev. 76, 301 (1949).
17. Schuch, A. F. and Sturdivant, J. H., J. Chem. Phys. 18, 145 (1950).
18. Owen, M., Ann. Physik, Ser. 4, 37, 657 (1912).
19. Trombe, F., Compt. Rend. 198, 1591 (1934).
20. La Blanchetais, C., Compt. Rend. 220, 392 (1945).

21. Foex, M., Compt. Rend. 219, 117 (1944).

22. James, N. R., Legvold, S., and Spedding, F. H., Phys. Rev. 88, 1092 (1952).

23. Kevane, C. J., Legvold, S., and Spedding, F. H., Phys. Rev. 91, 1372 (1953)

24. Parkinson, D. H., Simon, F. E., and Spedding, F. H., Proc. Roy. Soc. A 207, 137 (1951).

25. Loriers, J., Compt. Rend. 226, 1018 (1948).

26. Vogel, R. F., Anorg. Chem. 31, 277 (1917).

27. Hanaman, "Über der legierungen Habilitationsschrift" Wien (1915). Original not available for examination; reported by Loriers, J., Compt. Rend. 226, 1018 (1948).

28. Ahmann, D. H., Iowa State College J. Sci. 27, 120 (1953).

29. Gaume-Mahn, F., Compt. Rend. 241, 286 (1955).

30. Rossi, A., Atti. Acad. Nazl. Lincei 15, 298 (1932).

31. Rossi, A., Nature (London) 133, 174 (1934).

32. Klemm, W. and Bommer, H., Z. anorg. u. allgem. Chem. 231, 138 (1937).

33. Klemm, W. and Bommer, H., Z. anorg. u. allgem. Chem. 241, 264 (1939).

34. Johnson, R. G. and others, Unpublished Research, Iowa State College. Ames, Iowa (1953).

35. La Blanchetais, C., Compt. Rend. 234, 1353 (1952).

36. Quill, L. L., J. anorg. u. allgem. Chem. 208, 273 (1932).

37. Ellinger, F. H., J. Metals 7, 411 (1955).

38. Behrendt, D., Unpublished Research. Iowa State College. Ames, Iowa (1955).

39. Trombe, F. and Foex, M., Compt. Rend. 232, 63 (1951).

40. Bates, L. F. and others, Proc. Phys. Soc. (London) 68, 181 (1955).

41. Banister, J. R., Legvold, S., and Spedding, F. H., Phys. Rev. 94, 1140 (1954).

42. Urbain, G., Weiss, P., and Trombe, F., Compt. Rend. 200, 2132 (1935).

43. Elliott, J., Legvold, S., and Spedding, F. H., Phys. Rev. 91, 28 (1953).

44. Legvold, S., Spedding, F. H., Barson, F., and Elliott, J., Rev. Mod. Phys. 25, 129 (1953).

45. Griffel, M., Skochdopole, R. E., and Spedding, F. H., Phys. Rev. 93, 657 (1954).

46. Trombe, F. and Foes, M., Compt. Rend. 235, 42 (1952).

47. Thoburn, W. C., Rhodes, B. L., Johnson, R., Legvold, S., and Spedding, F. H., Unpublished Research. Iowa State College. Ames, Iowa (1956).

48. Elliott, J. F., Legvold, S., and Spedding, F. H., Phys. Rev. 94, 1143 (1954).

49. Trombe, F., Compt. Rend. 221, 19 (1945).

50. Trombe, F. and Foex, M., Compt. Rend. 235, 163 (1952).

51. Trombe, F., J. Phys. Radium 12, 222 (1951).

52. McLennan, J. C. and Monkman, R. J., Trans. Roy. Soc. Can. Sect. III 23, 255 (1929).

53. Elliott, J. F., Legvold, S., and Spedding, F. H., Phys. Rev. 100, 1595 (1955).

54. Koehler, W. C. and Wollan, R. O., Phys. Rev. 97, 1177 (1955).

55. Skochdopole, R. E., Griffel, M., and Spedding, F. H., J. Chem. Phys. 23, 2258 (1955).

56. Bommer, H., Z. anorg. Chem. 242, 277 (1939).

57. Bridgman, P. W., Proc. Am. Acad. Arts Sci. 83, 1 (1954).

58. Jenkins, F. A. and White, H. E., "Fundamentals of Optics" (McGraw-Hill Book Co., Inc., New York, 1950) p. 249.

59. Chiotti, P., Rev. Sci. Instr. 25, 876 (1954).

60. Work, R. N., J. Res. N.B.S. 47, 80 (1951).

61. Peck, E. R. and Obetz, S. W., J. Opt. Soc. Am. 43, 505 (1953).

62. Saunders, J. B., J. Res. N.B.S. 28, 51 (1942).

63. Esser, H. and Eusterbrock, H., Archiv Eisenhuttenw. 14, 341 (1941).

64. Dittenberger, W. and Gehrcke, H., Forsch. Arb. Ing-Wes. H.9, 60 (1903).

65. Nix, F. C. and MacNair, D., Phys. Rev. 60, 597 (1941).

66. Henning, F., Ann. Physik 22, 631 (1907).

67. Rosenbohm, E., Physica 5, 385 (1938).

68. Uffelman, F. L., Phil. Mag. 10, 633 (1930).

69. Eucken, A. and Dannoehl, W., Zeits. f. Elektrochemie 40, 814 (1934).

70. Spedding, F. H. and others, J. Am. Chem. Soc. 73, 4840 (1951).

71. Spedding, F. H. and others, Ind. Eng. Chem. 44, 553 (1952).

72. Spedding, F. H. and Daane, A. H., J. Am. Chem. Soc. 74, 2783 (1952).

73. Daane, A. H. and Spedding, F. H., J. Electrochem. Soc. 100, 442 (1953).

74. Daane, A. H., Dennison, D., and Spedding, F. H., J. Am. Chem. Soc. 75, 2272 (1953).

75. Andrade, E. N. da C., "Report of a Conference on Strength of Solids" (The Physical Society, London, 1948), p. 20.

76. Nabarro, F. R. N., "Report of a Conference on Strength of Solids" (The Physical Society, London, 1948), p. 75.

77. Orowan, E., J. West Scotland Iron and Steel Inst. (1947). Original not available for examination; reported by Betteridge, W. and Franklin, A. W., J. Inst. Metals 80, 147 (1951).

78. Betteridge, W. and Franklin, A. W., J. Inst. Metals 80, 147 (1951).

79. Bozorth, R. M., "Ferromagnetism" (D. Van Nostrand Co., New York, 1951), p. 444.

80. Zener, C. and Heikes, R. R., Rev. Mod. Phys. 25, 198 (1953).

81. Mott and Potter, Unpublished Research; reported by Nix, F. C. and MacNair, D., Phys. Rev. 60, 597 (1941).

82. Slater, J. C., Phys. Rev. 57, 744 (1940).

ACKNOWLEDGMENTS

The author is happy to express his appreciation to Dr. Sam Legvold and Dr. F. H. Spedding for suggesting this investigation and for their interest and assistance throughout the work. The author is also indebted to Dr. J. Powell for producing the pure rare earth salts needed, to Mr. R. Valetta for the painstaking task of casting the samples of rare earth metals used, to Mr. A. Read for designing parts of the electronic equipment, and to Mr. D. Strandburg for his assistance in calculating the results.

APPENDIX: EXPANSION DATA

Table 2a. Lanthanum, Run 1 (Warming)

Temp., °C	$\frac{\Delta L}{L_o} \times 10^3$	Temp., °C	$\frac{\Delta L}{L_o} \times 10^3$
41.4	0.017	313.1	0.824
47.0	0.052	318.9	0.744
53.0	0.077	329.0	0.789
61.8	0.117	357.3	1.001
72.3	0.171	385.6	1.231
84.6	0.243	410.6	1.436
97.6	0.326	436.9	1.652
113.0	0.419	463.0	1.879
128.6	0.501	490.9	2.134
147.4	0.595	518.8	2.411
165.9	0.707	547.5	2.710
184.9	0.824	574.9	3.002
206.7	0.971	603.4	3.244
231.2	1.136	629.4	3.585
254.7	1.295	655.3	3.887
279.6	1.461	680.4	4.182
297.7	1.578	705.4	4.471
303.5	1.543	736.2	4.785
306.8	1.350	760.6	4.962
309.5	1.072	779.5	5.060

Table 2b. Lanthanum, Run 1 (Cooling)

Temp., °C	$\frac{\Delta L}{L_o} \times 10^3$	Temp., °C	$\frac{\Delta L}{L_o} \times 10^3$
775.4	4.924	366.5	0.366
762.8	4.724	342.4	0.167
748.8	4.506	317.3	-0.033
726.3	4.190	293.9	-0.214
704.7	3.897	268.7	-0.403
681.9	3.602	245.7	-0.578
657.3	3.296	234.7	-0.652
637.4	3.031	222.8	-0.498
615.5	2.776	207.2	-0.405
591.4	2.503	181.3	-0.461
567.1	2.285	161.7	-0.550
542.4	2.022	143.4	-0.639
516.9	1.747	125.4	-0.732
492.9	1.500	108.5	-0.814
469.0	1.280	94.3	-0.872
442.6	1.036	80.8	-0.923
416.1	0.797	71.0	-0.962
390.8	0.582		

Table 2c. Lanthanum, Run 2 (Warming)

Temp., °C	$\frac{\Delta L}{L_o} \times 10^3$	Temp., °C	$\frac{\Delta L}{L_o} \times 10^3$
26.5	0.011	472.6	2.330
32.4	0.030	500.4	2.586
38.5	0.063	528.1	2.862
48.8	0.115	555.2	3.148
59.2	0.175	587.9	3.521
71.8	0.243	616.7	3.858
84.7	0.310	643.8	4.166
99.3	0.390	670.8	4.479
115.5	0.483	696.0	4.780
135.4	0.600	724.8	5.126
157.1	0.729	755.2	5.502
177.0	0.852	784.0	5.854
198.8	0.993	814.4	6.118
221.3	1.146	826.0	6.157
244.6	1.312	839.9	6.074
269.5	1.488	849.8	6.017
292.6	1.636	855.2	5.880
300.0	1.666	858.3	5.686
308.6	1.562	860.6	5.519
311.7	1.341	862.3	5.353
314.5	1.148	863.9	5.186
320.0	1.028	864.7	5.019
344.9	1.194	865.7	4.853
370.7	1.405	865.0	4.685
394.8	1.627	864.9	4.517
419.7	1.842	864.7	4.350
448.1	2.093	864.5	4.182

Table 3a. Cerium, Run 1 (Cooling)

Temp., °C	$\frac{\Delta L}{L_o} \times 10^3$	Temp., °C	$\frac{\Delta L}{L_o} \times 10^3$
698.2	3.860	275.5	0.619
690.4	3.785	252.5	0.478
674.4	3.626	235.3	0.365
653.7	3.400	212.3	0.242
627.9	3.183	190.7	0.109
606.6	2.981	171.7	-0.011
583.8	2.801	151.4	-0.138
559.9	2.608	134.1	-0.251
534.9	2.412	117.0	-0.363
508.6	2.213	101.4	-0.474
483.3	2.012	84.5	-0.579
454.4	1.815	74.1	-0.669
425.1	1.605	63.6	-0.746
397.9	1.426	53.5	-0.818
373.3	1.259	46.2	-0.875
346.9	1.080	41.2	-0.914
323.1	0.926	35.4	-0.964
298.6	0.766	33.0	-1.008

Table 3b. Cerium, Run 2 (Warming)

Temp., °C	$\frac{\Delta L}{L_o} \times 10^3$	Temp., °C	$\frac{\Delta L}{L_o} \times 10^3$
21.8	0.008	318.2	1.956
27.3	0.071	346.4	2.137
34.8	0.128	374.9	2.324
43.7	0.199	401.9	2.504
54.2	0.282	428.2	2.682
66.0	0.373	455.6	2.874
78.2	0.463	481.1	3.057
93.2	0.567	508.0	3.253
110.4	0.686	535.4	3.458
129.5	0.810	564.9	3.693
149.1	0.936	593.3	3.917
169.1	1.056	621.7	4.154
191.2	1.184	646.0	4.364
215.4	1.326	671.5	4.593
240.4	1.474	699.5	4.822
265.9	1.629	721.9	4.952
291.7	1.790	725.5	4.924

Table 3c. Cerium, Run 2 (Cooling)

Temp., °C	$\frac{\Delta L}{L_o} \times 10^3$	Temp., °C	$\frac{\Delta L}{L_o} \times 10^3$
716.6	4.526	306.8	1.230
706.4	4.371	283.4	1.082
683.5	4.167	259.9	0.935
668.3	3.974	238.2	0.801
643.5	3.733	215.7	0.660
616.2	3.486	192.8	0.520
587.2	3.243	172.8	0.393
560.9	3.025	152.6	0.267
535.3	2.819	132.0	0.141
509.8	2.624	114.4	0.028
482.9	2.422	98.6	-0.077
455.7	2.226	83.1	-0.181
430.0	2.042	69.7	-0.279
406.5	1.877	55.5	-0.382
382.8	1.724	41.8	-0.491
358.8	1.564	33.0	-0.561
332.1	1.390	29.5	-0.593

Table 4a. Praseodymium, Run 1 (Cooling)

Temp., °C	$\frac{\Delta L}{L_o} \times 10^3$	Temp., °C	$\frac{\Delta L}{L_o} \times 10^3$
826.5	3.676	416.6	-1.407
810.3	2.965	389.9	-1.577
793.0	2.321	364.3	-1.736
790.5	2.236	336.3	-1.906
787.9	2.129	312.4	-2.048
783.0	2.021	286.0	-2.202
794.8	2.428	262.2	-2.338
771.3	1.756	239.4	-2.463
751.9	1.441	214.0	-2.601
729.2	1.145	192.0	-2.714
703.5	0.876	170.9	-2.822
680.3	0.648	150.7	-2.424
655.6	0.415	132.8	-3.013
630.7	0.192	114.0	-3.103
604.3	-0.032	97.2	-3.181
579.4	-0.236	82.6	-3.246
552.0	-0.448	67.6	-3.312
524.2	-0.659	48.0	-3.401
497.2	-0.858	34.4	-3.460
469.1	-1.054	24.2	-3.502
442.8	-1.233		

Table 4b. Praseodymium, Run 2 (Warming)

Temp., °C	$\frac{\Delta L}{L_o} \times 10^3$	Temp., °C	$\frac{\Delta L}{L_o} \times 10^3$
22.9	0.009	402.1	2.034
26.9	0.027	431.4	2.226
31.6	0.050	458.9	2.419
38.2	0.079	484.9	2.603
48.5	0.126	513.1	2.815
58.2	0.173	544.7	3.061
71.5	0.233	575.4	3.310
84.0	0.293	602.7	3.535
99.8	0.364	630.1	3.776
115.7	0.437	659.2	4.039
135.0	0.527	687.6	4.301
155.3	0.624	715.2	4.568
175.6	0.725	747.9	4.864
197.8	0.840	778.4	5.132
220.8	0.960	789.7	5.227
246.5	1.104	792.0	5.266
272.8	1.247	797.4	5.305
300.4	1.405	807.9	5.357
324.3	1.551	816.6	5.377
350.4	1.705	833.0	5.294
375.2	1.858		

Table 4c. Praseodymium, Run 2 (Cooling)

Temp., °C	$\frac{\Delta L}{L_o} \times 10^3$	Temp., °C	$\frac{\Delta L}{L_o} \times 10^3$
831.1	4.931	463.8	0.601
818.9	4.522	438.4	0.433
798.0	4.066	412.9	0.275
794.2	3.979	386.2	0.103
792.0	3.872	360.3	-0.055
789.6	3.780	336.7	-0.198
786.4	3.683	310.2	-0.341
782.0	3.575	288.5	-0.477
776.2	3.444	265.2	-0.609
769.8	3.341	242.2	-0.734
764.2	3.254	218.2	-0.861
759.2	3.177	195.9	-0.976
754.9	3.111	173.3	-1.090
727.1	2.764	152.6	-1.187
698.5	2.476	133.0	-1.278
669.6	2.218	114.0	-1.362
644.9	1.979	96.8	-1.441
618.6	1.755	81.5	-1.507
592.5	1.541	69.0	-1.561
564.8	1.325	48.4	-1.651
539.6	1.137	35.6	-1.704
514.2	0.954	27.2	-1.734
489.2	0.776		

Table 5a. Neodymium, Run 1 (Cooling)

Temp., °C	$\frac{\Delta L}{L_o} \times 10^3$	Temp., °C	$\frac{\Delta L}{L_o} \times 10^3$
911.4	6.580	464.4	0.951
896.2	6.324	438.9	0.725
876.5	5.991	413.7	0.508
870.7	5.888	388.0	0.291
867.7	5.754	363.1	0.090
865.2	5.594	337.7	-0.111
862.9	5.433	311.8	-0.318
857.5	5.298	287.2	-0.508
851.6	5.237	262.5	-0.693
827.1	4.871	238.4	-0.873
805.6	4.527	215.9	-1.051
779.1	4.165	192.6	-1.224
752.0	3.830	171.7	-1.369
724.0	3.526	149.9	-1.514
700.2	3.230	130.2	-1.642
674.7	2.943	112.5	-1.758
648.0	2.661	95.6	-1.867
623.4	2.390	81.8	-1.959
596.6	2.150	68.2	-2.051
572.9	1.926	56.3	-2.136
546.8	1.686	40.0	-2.239
517.1	1.437	27.9	-2.319
491.2	1.184		

Table 5b. Neodymium, Run 2 (Warming)

Temp., °C	$\frac{\Delta L}{L_o} \times 10^3$	Temp., °C	$\frac{\Delta L}{L_o} \times 10^3$
24.2	0.009	384.1	2.660
28.1	0.043	416.9	2.919
33.3	0.082	447.7	3.171
40.8	0.133	475.7	3.426
49.4	0.190	503.7	3.690
59.6	0.259	534.0	3.956
72.0	0.344	563.0	4.225
86.3	0.441	588.3	4.481
102.8	0.551	612.0	4.730
119.8	0.666	635.6	4.990
138.9	0.793	662.8	5.262
157.8	0.921	687.2	5.565
178.3	1.060	714.5	5.905
200.8	1.217	753.8	6.208
225.3	1.396	779.0	6.527
250.6	1.592	803.5	6.830
276.0	1.788	828.0	7.143
300.8	1.983	853.1	7.519
326.9	2.190	865.8	7.674
356.0	2.426	882.9	7.623

Table 5c. Neodymium, Run 2 (Cooling)

Temp., °C	$\frac{\Delta L}{L_o} \times 10^3$	Temp., °C	$\frac{\Delta L}{L_o} \times 10^3$
885.1	7.221	469.3	2.254
874.0	7.030	440.0	1.988
870.5	6.901	410.9	1.764
867.8	6.768	383.7	1.535
866.7	6.682	360.0	1.341
864.3	6.548	335.5	1.129
860.3	6.441	309.0	0.917
850.0	6.287	284.4	0.721
828.0	5.995	260.6	0.537
803.0	5.655	238.9	0.369
777.0	5.316	216.3	0.202
753.6	5.030	193.2	0.034
729.1	4.749	172.0	-0.106
707.4	4.507	151.6	-0.239
684.7	4.247	132.2	-0.367
654.9	3.969	115.3	-0.483
626.8	3.723	99.1	-0.587
604.5	3.480	83.5	-0.690
576.8	3.223	70.4	-0.776
555.0	2.984	49.0	-0.914
527.5	2.748	35.7	-0.999
500.4	2.526	29.0	-1.050

Table 6a. Gadolinium, Run 1 (Cooling)

Temp., °C	$\frac{\Delta L}{L_o} \times 10^3$	Temp., °C	$\frac{\Delta L}{L_o} \times 10^3$
940.2	8.945	431.8	2.804
932.9	8.806	404.8	2.568
923.1	8.623	378.8	2.342
910.0	8.386	353.2	2.122
888.3	8.019	331.2	1.935
868.0	7.690	307.9	1.742
846.0	7.355	285.0	1.555
825.0	7.047	262.0	1.373
803.8	6.749	237.2	1.180
782.0	6.456	215.9	1.019
756.0	6.119	194.1	0.859
731.4	5.815	173.7	0.711
706.0	5.511	154.1	0.574
680.9	5.222	134.2	0.442
655.0	4.938	117.8	0.338
626.9	4.642	101.2	0.209
602.4	4.395	75.1	0.086
570.9	4.086	61.6	-0.016
540.8	3.799	44.1	-0.060
512.6	3.531	31.0	-0.093
484.5	3.276	26.9	-0.099
458.0	3.035		

Table 6b. Gadolinium, Run 2 (Warming)

Temp., °C	$\frac{\Delta L}{L_o} \times 10^3$	Temp., °C	$\frac{\Delta L}{L_o} \times 10^3$
-143.3	0.027	301.4	1.812
-107.2	0.149	327.5	2.027
-89.1	0.226	353.9	2.248
-74.5	0.278	379.8	2.468
-61.6	0.311	404.5	2.683
-37.5	0.336	434.6	2.942
-18.5	0.309	467.0	3.218
-6.5	0.265	495.9	3.476
10.4	0.140	522.9	3.721
16.4	0.064	550.8	3.987
25.8	0.015	579.0	4.258
32.2	0.018	609.2	4.561
43.4	0.050	642.4	4.906
55.4	0.097	671.5	5.218
69.7	0.167	701.0	5.550
85.3	0.253	733.7	5.931
101.7	0.350	761.0	6.268
121.2	0.471	789.8	6.632
140.6	0.597	815.0	6.969
160.4	0.735	842.5	7.359
181.6	0.888	867.6	7.732
205.0	1.066	890.0	8.068
227.4	1.236	911.6	8.407
250.4	1.413	931.8	8.742
275.3	1.607		

Table 6c. Gadolinium, Run 2 (Cooling)

Temp., °C	$\frac{\Delta L}{L_o} \times 10^3$	Temp., °C	$\frac{\Delta L}{L_o} \times 10^3$
932.3	8.742	421.2	2.556
917.4	8.479	393.0	2.309
900.7	8.177	366.5	2.078
877.2	7.789	339.8	1.851
855.1	7.427	315.4	1.647
831.2	7.060	289.7	1.437
805.5	6.682	264.8	1.233
783.3	6.377	241.6	1.051
757.4	6.041	219.2	0.869
726.2	5.687	196.0	0.708
705.7	5.395	175.3	0.563
679.3	5.090	154.1	0.411
656.3	4.839	134.1	0.279
632.8	4.582	116.0	0.164
606.3	4.302	100.2	0.067
581.1	4.049	84.3	-0.026
555.5	3.790	71.5	-0.095
527.3	3.519	58.9	-0.159
502.3	3.285	49.7	-0.200
474.8	3.028	35.6	-0.248
448.9	2.793		

Table 7a. Terbium, Run 1 (Cooling)

Temp., °C	$\frac{\Delta L}{L_o} \times 10^3$	Temp., °C	$\frac{\Delta L}{L_o} \times 10^3$
951.7	10.357	397.4	3.412
931.9	10.052	372.3	3.158
915.4	9.800	351.6	2.938
893.0	9.481	326.0	2.688
870.1	9.115	301.3	2.439
848.2	8.834	277.9	2.212
823.5	8.467	255.1	1.980
801.4	8.143	229.4	1.752
776.7	7.798	208.1	1.553
750.9	7.452	185.7	1.348
725.2	7.116	165.6	1.166
699.0	6.765	145.2	0.985
671.8	6.451	125.9	0.819
644.0	6.120	108.2	0.672
613.8	5.734	93.0	0.547
582.2	5.400	79.7	0.428
555.9	5.101	65.6	0.315
529.9	4.817	57.0	0.247
503.2	4.526	48.3	0.180
476.9	4.246	40.3	0.117
449.2	3.954	32.0	0.060
421.4	3.661	25.1	0.010

Table 7b. Terbium, Run 2 (Warming)

Temp., °C	$\frac{\Delta L}{L_o} \times 10^3$	Temp., °C	$\frac{\Delta L}{L_o} \times 10^3$
-141.2	0.313	278.4	2.175
-129.8	0.363	304.3	2.425
-103.1	0.411	331.9	2.692
-93.2	0.410	360.2	2.976
-73.8	0.330	386.9	3.252
-60.1	0.172	413.4	3.534
-52.5	-0.013	440.9	3.821
-46.8	-0.172	470.2	4.136
-40.7	-0.320	500.8	4.471
-33.0	-0.318	530.3	4.743
-19.5	-0.272	559.8	5.071
-5.7	-0.199	586.1	5.371
12.1	-0.086	615.0	5.724
27.8	0.027	645.1	6.104
40.7	0.123	671.4	6.461
54.6	0.225	699.8	6.862
69.7	0.341	728.0	7.282
84.3	0.457	756.4	7.731
101.9	0.600	783.1	8.167
121.9	0.764	811.9	8.658
140.2	0.918	838.4	9.127
160.4	1.094	864.6	9.538
181.2	1.282	889.7	9.884
204.4	1.492	911.8	10.180
228.4	1.714	938.2	10.549
252.3	1.936		

Table 7c. Terbium, Run 2 (Cooling)

Temp., °C	$\frac{\Delta L}{L_o} \times 10^3$	Temp., °C	$\frac{\Delta L}{L_o} \times 10^3$
938.4	10.549	687.1	6.888
918.8	10.253	660.2	6.552
901.0	9.990	633.0	6.221
879.0	9.672	607.3	5.917
859.0	9.386	581.1	5.607
837.8	9.084	556.7	5.383
813.6	8.643	529.6	5.093
788.9	8.255	504.0	4.798
765.6	7.915	476.8	4.506
739.5	7.566	448.5	4.224
714.0	7.229	421.2	3.937

Table 8a. Dysprosium, Run 1 (Cooling)

Temp., °C	$\frac{\Delta L}{L_o} \times 10^3$	Temp., °C	$\frac{\Delta L}{L_o} \times 10^3$
932.0	9.946	415.6	2.992
919.8	9.774	386.6	2.664
901.8	9.508	361.4	2.378
882.6	9.195	336.6	2.105
861.4	8.886	310.3	1.813
838.0	8.537	286.8	1.557
813.6	8.176	262.6	1.300
788.2	7.808	241.3	1.075
764.3	7.453	219.5	0.843
739.2	7.092	196.7	0.605
713.5	6.737	175.4	0.386
687.4	6.358	154.9	0.179
659.7	5.967	135.2	-0.022
635.6	5.646	117.9	-0.192
609.5	5.307	101.2	-0.356
584.6	4.991	86.0	-0.518
558.1	4.662	72.8	-0.641
530.1	4.320	52.2	-0.841
503.6	4.001	39.3	-0.961
476.4	3.693	28.1	-1.058
446.6	3.326		

Table 8b. Dysprosium, Run 2 (Warming)

Temp., °C	$\frac{\Delta L}{L_o} \times 10^3$	Temp., °C	$\frac{\Delta L}{L_o} \times 10^3$
25.4	0.010	436.3	4.278
28.2	0.040	466.4	4.630
34.3	0.089	493.4	4.960
41.6	0.149	520.8	5.303
50.8	0.234	547.1	5.633
60.6	0.325	578.5	6.011
72.9	0.440	610.0	6.405
87.0	0.571	639.8	6.798
101.9	0.719	666.0	7.183
120.2	0.891	696.9	7.645
140.5	1.085	726.1	8.100
160.0	1.281	758.4	8.608
182.2	1.501	786.2	9.017
204.4	1.727	818.4	9.474
228.3	1.965	846.9	9.867
252.3	2.216	871.4	10.188
278.7	2.491	894.9	10.550
304.2	2.772	921.5	10.872
328.2	3.051	950.6	11.265
353.2	3.331	970.0	11.543
377.7	3.610	989.8	11.807
405.1	3.920	1001.3	11.962

Table 5c. Dysprosium, Run 2 (Cooling)

Temp., °C	$\frac{\Delta L}{L_o} \times 10^3$	Temp., °C	$\frac{\Delta L}{L_o} \times 10^3$
1000.0	11.944	442.8	4.311
982.1	11.723	415.8	3.984
961.5	11.403	386.4	3.656
943.5	11.124	360.2	3.358
919.4	10.762	334.0	3.066
895.8	10.401	308.6	2.792
871.8	10.045	284.2	2.524
844.0	9.636	258.8	2.255
822.6	9.304	236.2	2.011
800.8	9.001	213.2	1.772
781.0	8.711	190.8	1.535
756.2	8.360	169.9	1.321
731.2	7.993	150.1	1.120
702.8	7.597	130.3	0.919
677.7	7.223	112.0	0.736
656.8	6.920	95.9	0.578
630.7	6.576	80.8	0.427
605.7	6.248	68.6	0.306
577.9	5.941	52.9	0.160
550.6	5.560	41.1	0.040
526.2	5.263	30.4	-0.068
499.7	4.947	26.4	-0.105
474.6	4.623		

Table 9a. Erbium, Run 1 (Cooling)

Temp., °C	$\frac{\Delta L}{L_o} \times 10^3$	Temp., °C	$\frac{\Delta L}{L_o} \times 10^3$
937.7	9.714	401.5	2.262
926.5	9.556	374.6	1.968
912.5	9.344	350.0	1.700
897.3	9.102	326.2	1.450
873.8	8.667	303.2	1.206
850.5	8.239	281.5	0.981
829.8	7.883	257.8	0.737
806.0	7.489	235.4	0.511
782.0	7.102	212.8	0.280
762.5	6.770	192.4	0.067
735.6	6.400	170.0	-0.146
711.8	6.037	150.2	-0.339
682.6	5.642	130.8	-0.533
658.1	5.284	113.3	-0.701
629.2	4.912	97.1	-0.869
598.7	4.557	80.3	-1.019
569.8	4.184	67.8	-1.145
539.5	3.828	56.2	-1.254
507.7	3.458	47.1	-1.347
479.2	3.125	35.4	-1.458
453.3	2.834	26.3	-1.545
427.4	2.542		

Table 9b. Erbium, Run 2 (Warming)

Temp., °C	$\frac{\Delta L}{L_o} \times 10^3$	Temp., °C	$\frac{\Delta L}{L_o} \times 10^3$
25.4	0.010	401.0	3.807
32.3	0.083	431.2	4.132
39.7	0.155	461.2	4.461
49.6	0.250	488.9	4.777
60.0	0.356	519.4	5.123
72.2	0.473	548.4	5.468
85.6	0.604	575.8	5.806
100.7	0.753	608.0	6.198
117.1	0.909	637.2	6.576
137.2	1.103	665.1	6.954
157.0	1.302	695.3	7.368
177.0	1.496	723.1	7.773
195.5	1.684	750.6	8.195
216.0	1.898	779.8	8.650
241.6	2.142	806.9	9.110
267.8	2.412	829.4	9.485
292.3	2.680	850.7	9.873
317.5	2.937	880.2	10.440
341.7	3.193	907.0	10.970
369.8	3.488	936.0	11.425

Table 9c. Erbium, Run 2 (Cooling)

Temp., °C	$\frac{\Delta L}{L_o} \times 10^3$	Temp., °C	$\frac{\Delta L}{L_o} \times 10^3$
929.6	11.334	389.8	3.770
912.2	11.066	364.5	3.489
888.3	10.678	339.6	3.227
873.9	10.360	313.8	2.951
853.9	10.003	289.6	2.701
832.6	9.623	264.3	2.444
808.6	9.217	241.8	2.212
783.2	8.811	219.0	1.980
758.0	8.442	195.8	1.748
734.2	8.060	174.4	1.536
706.8	7.648	154.0	1.335
681.2	7.289	134.5	1.138
655.6	6.931	116.3	0.967
628.0	6.565	99.6	0.804
602.8	6.242	84.0	0.649
576.8	5.917	69.8	0.507
550.4	5.598	54.1	0.363
523.3	5.278	44.3	0.265
495.7	4.951	38.2	0.201
469.0	4.647	29.4	0.123
441.3	4.337	25.9	0.092
416.2	4.057		

Table 10a. Ytterbium, Run 1 (Cooling)

Temp., °C	$\frac{\Delta L}{L_o} \times 10^3$	Temp., °C	$\frac{\Delta L}{L_o} \times 10^3$
760.8	20.816	411.8	10.352
746.1	20.517	386.4	9.568
739.9	20.356	360.6	8.761
734.2	20.269	333.7	7.987
732.9	20.184	308.4	7.237
731.3	20.099	283.2	6.482
728.6	19.934	259.2	6.021
718.5	19.642	235.8	5.497
707.8	19.452	210.3	4.849
699.0	19.267	188.2	4.259
688.6	19.004	167.6	3.688
663.1	18.470	145.9	3.127
637.5	17.781	127.0	2.625
615.6	17.036	116.4	2.145
591.4	16.217	93.7	1.704
568.5	15.438	79.3	1.313
543.0	14.584	66.7	0.973
518.0	13.757	51.8	0.576
491.8	12.901	40.4	0.288
462.9	11.980	29.8	0.001
437.2	11.169		

Table 10b. Ytterbium, Run 2 (Warming)

Temp., °C	$\frac{\Delta L}{L_o} \times 10^3$	Temp., °C	$\frac{\Delta L}{L_o} \times 10^3$
24.1	0.010	432.8	11.286
30.8	0.181	461.0	12.165
37.8	0.365	486.8	12.992
45.9	0.583	517.3	13.967
55.8	0.852	544.7	14.861
67.3	1.151	574.4	15.835
80.4	1.513	603.9	16.824
95.8	1.927	629.8	17.726
112.8	2.381	656.0	18.663
131.5	2.820	684.5	19.684
151.4	3.299	696.3	20.033
171.0	3.807	702.8	20.285
192.1	4.355	709.2	20.541
216.2	5.000	715.1	20.842
240.8	5.654	720.2	21.109
267.6	6.369	725.9	21.393
293.2	7.084	734.3	21.612
319.9	7.828	749.8	21.545
349.1	8.692	767.9	21.496
376.3	9.532	770.9	21.283
405.2	10.418		